

STABILITY AND SUPERCONVERGENCE OF A SPECIAL Q_1 -FINITE VOLUME ELEMENT SCHEME OVER QUADRILATERAL MESHES

YANHUI ZHOU

Abstract. This paper studied the stability and superconvergence of a special isoparametric bilinear finite volume element scheme for anisotropic diffusion problems over quadrilateral meshes, where the scheme is obtained by employing the edge midpoint rule to approximate the line integrals in classical Q_1 -finite volume element method. It can be checked that the scheme is identical to the standard five-point difference scheme for a special case. By element analysis approach, we suggest a sufficient condition to guarantee the stability of the scheme. This condition has an analytic expression, which covers the traditional $h^{1+\gamma}$ -parallelogram and some trapezoidal meshes with any full anisotropic diffusion tensor. Moreover, based on the h^2 -uniform quadrilateral mesh assumption, we proved the superconvergence $|u_I - u_h|_1 = \mathcal{O}(h^2)$, where u_I is the isoparametric bilinear interpolation of exact solution u , and u_h is the numerical solution. As a by product, we obtained the optimal H^1 and L^2 error estimates. Finally, the theoretical results are verified by some numerical experiments.

Key words. Q_1 -finite volume element scheme, stability, superconvergence, H^1 and L^2 error estimates, anisotropic diffusion equation.

1. Introduction

The finite volume element (FVE) method (FVEM) is also called as generalized difference method [1] or box method [2]. Since FVEM possesses local conservation law and other advantages, it has been attracted many researchers attention, see the book [3] and review papers [4, 5]. For the Poisson equation, the element stiffness matrix of linear FVEM is identical to the corresponding linear finite element method (FEM) on arbitrary triangular meshes, and the coercivity result follows [6, 7]. Under the coercivity result, the optimal H^1 error analysis can be established by a standard technique. Further, [8, 9] proved the optimal L^2 error estimate on general triangular meshes, and [10, 11] applied linear FVEM to some more complicated problems. More relevant studies of high order FVEMs are presented in [12, 13, 14, 15, 16] and so on.

However, the development of standard isoparametric bilinear FVEM (Q_1 -FVEM) over quadrilateral meshes is still lags far behind. To ensure the coercivity result, most work require quasi-parallelogram mesh condition [17, 18, 19]. In 2020, [20] suggested a sufficient condition to guarantee the coercivity, and this condition covers the traditional quasi-parallelogram mesh, but regrettably it not cover arbitrary trapezoidal mesh. Once the coercivity result is established, then the optimal H^1 error analysis of classical Q_1 -FVEM is trival. On the other hand, by approximating the line integrals in classical Q_1 -FVEM at geometric center of the quadrilateral, [21] constructed a symmetric Q_1 -FVE scheme, such that the global stiffness matrix is symmetric. Recently, [22], [23] and [24] employed trapezoidal, midpoint and Simpson rules to approximate the line integrals respectively, and the coercivity results of these new schemes are validated over traditional quasi-parallelogram and some

trapezoidal meshes. Further, based on Wachspress generalized barycentric coordinate, in 2023 [25] designed a polygonal FVEM to solve the anisotropic diffusion problems and presented an optimal H^1 error estimate. For more studies of FVEM over quadrilateral meshes, we refer the readers to [26, 27, 28, 29] for incomplete references.

Under the coercivity result and H^1 error estimate, we may investigate the L^2 error and superconvergence of FVEM solution. By employing the barycenters of triangles to construct the dual mesh, [30] shown that the difference between linear FEM solution and FVEM solution over triangular mesh is of second order in energy norm. On the other hand, by using Taylor's expansion, [21] presented the optimal L^2 error estimate and superconvergence of a special symmetric Q_1 -FVE scheme over uniform rectangular meshes. Assume that the quadrilateral mesh is h^2 -uniform, and by using the geometric centers of quadrilaterals to construct the dual mesh, [31] proved that the difference between classical Q_1 -FVEM solution and the interpolation of exact solution is also of second order in energy norm. More studies of the error analysis can be found in [32, 33, 34, 35] and so on.

In this paper, we employ the value at edge midpoint to approximate the line integrals in classical Q_1 -FVEM for solving anisotropic diffusion problems on general convex quadrilateral meshes. By element analysis approach, we suggest a sufficient condition to ensure the stability. This sufficient condition has an analytic expression, which only involves the anisotropic diffusion coefficient and the geometry of mesh. This leads to that for any full diffusion tensor and convex quadrilateral mesh, we can directly judge whether this sufficient condition is satisfied. More interesting is that, this condition covers the traditional $h^{1+\gamma}$ -parallelogram and some trapezoidal meshes with full anisotropic diffusion coefficient.

To study the superconvergence of the error $u_I - u_h$ in energy norm, we decompose it into two parts by using the coercivity result. The first part is the error $u_I - u$, then under h^2 -uniform quadrilateral mesh assumption and the superconvergence of bilinear interpolation on two adjacent quadrilateral elements, this error can be analyzed by some analysis techniques. Moreover, by Taylor's expansion, we can analyze the second part $u - u_h$. Thanks to these findings, we obtain the second order superconvergence result. As a result, we get that u_h converges to u with optimal convergence rates 1 and 2 under H^1 and L^2 norms, and the superconvergence results of u_h at geometric centers, interior vertices and edge midpoints which are all second order in an average gradient norm. We mention that [17] has pointed out that, if we use the edge midpoint rule to approximate the line integrals, then in some special cases, the new scheme is identical to the standard five-point difference scheme. However, its theoretical analysis has not been established. Thus, the novelty of this paper is that, under some mesh assumptions, we presented the stability and superconvergence for the special scheme.

The rest of this paper is organized as follows. In Section 2, we present a special isoparametric bilinear finite volume element scheme over general convex quadrilateral meshes. The stability and superconvergence results of the constructed scheme are shown in Sections 3 and 4 respectively. Some numerical experiments are reported in Section 5 to verify the theoretical results, and the conclusion is given in Section 6. In Section 8 (Appendix A), we give some lemmas that available in the literature. Some discussions for the assumption **(A1)** are presented in Section 9 (Appendix B).

Throughout the paper, C will be denote a generic constant that could change from one occurrence to the other. To avoid repetition, we sometimes write " $A \lesssim B$ "

to indicate that A can be bounded by B multiplied by a constant irrelative to the parameters which A and B may depend on. Analogously, “ $A \gtrsim B$ ” implies that B can be bounded by A , while “ $A \sim B$ ” stands for the fact that we have both “ $A \lesssim B$ ” and “ $B \lesssim A$ ”.

2. The Q_1 -FVEM-EM scheme

2.1. Models, meshes and spaces. Solve the following second order elliptic boundary value problem

$$\begin{aligned} (1) \quad & -\nabla \cdot (\Lambda \nabla u) = f, \quad \text{in } \Omega, \\ (2) \quad & u = 0, \quad \text{on } \partial\Omega, \end{aligned}$$

where $\Omega \subset \mathbb{R}^2$ is an open bounded connected polygonal domain, $f \in L^2(\Omega)$ is the source term, $\Lambda(\mathbf{x})$ is a 2×2 symmetric and positive definite matrix, i.e., there exist two positive constants $\underline{\lambda}$ and $\bar{\lambda}$ such that

$$(3) \quad \underline{\lambda} \|\mathbf{v}\|^2 \leq \mathbf{v}^T \Lambda \mathbf{v} \leq \bar{\lambda} \|\mathbf{v}\|^2, \quad \forall \mathbf{v} \in \mathbb{R}^2, \quad \forall \mathbf{x} = (x, y)^T \in \Omega,$$

and $\|\mathbf{v}\|$ denotes the Euclidean norm of vector \mathbf{v} . For simplicity, in the following analysis we only consider the homogeneous Dirichlet boundary condition and suppose that the diffusion coefficient Λ is a constant matrix on Ω .

Assume that Ω is divided into a finite number of non-overlapped and strictly convex quadrilateral elements that form the so-called *primary mesh* \mathcal{T}_h , namely $\Omega = \cup\{K : K \in \mathcal{T}_h\}$ with $h = \max_{K \in \mathcal{T}_h} h_K$ is the mesh size and h_K is diameter of K . Further, let \mathcal{T}_h be a *conform* mesh, i.e., the intersection of any two different quadrilateral elements is a common edge or a common vertex or empty. For any $K = \square \mathbf{x}_1 \mathbf{x}_2 \mathbf{x}_3 \mathbf{x}_4$, assume that \mathbf{y}_i is the midpoint of edge $\mathbf{x}_i \mathbf{x}_{i+1}$, $i = 1, 2, 3, 4$, here and hereafter i denotes, without special mention, a periodic index with period 4. In other words, we have $\mathbf{x}_5 = \mathbf{x}_1$. Denote \mathcal{N}_K , \mathcal{E}_K and \mathcal{M}_K as the set of four vertices \mathbf{x}_i , four edges $\mathbf{x}_i \mathbf{x}_{i+1}$ and four midpoints \mathbf{y}_i of K , respectively. Then, we can define

$$\mathcal{N}_h = \bigcup_{K \in \mathcal{T}_h} \mathcal{N}_K, \quad \mathcal{E}_h = \bigcup_{K \in \mathcal{T}_h} \mathcal{E}_K, \quad \mathcal{M}_h = \bigcup_{K \in \mathcal{T}_h} \mathcal{M}_K,$$

and

$$\mathcal{N}_h^\circ = \mathcal{N}_h \setminus \partial\Omega, \quad \mathcal{E}_h^\circ = \mathcal{E}_h \setminus \partial\Omega, \quad \mathcal{M}_h^\circ = \mathcal{M}_h \setminus \partial\Omega$$

as the set of all vertices, edges, midpoints of edges and interior vertices, interior edges, midpoints of interior edges of \mathcal{T}_h , respectively.

Suppose that $\hat{K} = \square \hat{\mathbf{x}}_1 \hat{\mathbf{x}}_2 \hat{\mathbf{x}}_3 \hat{\mathbf{x}}_4 = [-1, 1]^2$ is a reference square element locates on the (ξ, η) plane, where the coordinate of $\hat{\mathbf{x}}_i$ is given by

$$\hat{\mathbf{x}}_1 = (-1, -1)^T, \quad \hat{\mathbf{x}}_2 = (1, -1)^T, \quad \hat{\mathbf{x}}_3 = (1, 1)^T, \quad \hat{\mathbf{x}}_4 = (-1, 1)^T.$$

Here and hereafter, we will not distinguish between a point and its position vector, they share the same symbol. Let

$$\hat{\phi}_1 = \frac{(1-\xi)(1-\eta)}{4}, \hat{\phi}_2 = \frac{(1+\xi)(1-\eta)}{4}, \hat{\phi}_3 = \frac{(1+\xi)(1+\eta)}{4}, \hat{\phi}_4 = \frac{(1-\xi)(1+\eta)}{4}$$

be the four bilinear nodal basis functions which defined on \hat{K} . Obviously, we have $\hat{\phi}_i(\hat{\mathbf{x}}_j) = \delta_{ij}$, where δ_{ij} denotes the Kronecker delta, namely $\delta_{ij} = 1$ if $i = j$, $\delta_{ij} = 0$ if $i \neq j$. For any strictly convex quadrilateral K , there exists a unique invertible bilinear mapping \mathcal{J}_K which maps \hat{K} onto K , and satisfying $\mathcal{J}_K(\hat{\mathbf{x}}_i) = \mathbf{x}_i$, $i = 1, 2, 3, 4$. In particular, \mathcal{J}_K has the following expression

$$(4) \quad \mathcal{J}_K(\xi, \eta) = \mathbf{x}_K + \frac{1}{2}(\mathbf{m}_1 \xi + \mathbf{m}_2 \eta + \mathbf{m}_K \xi \eta),$$

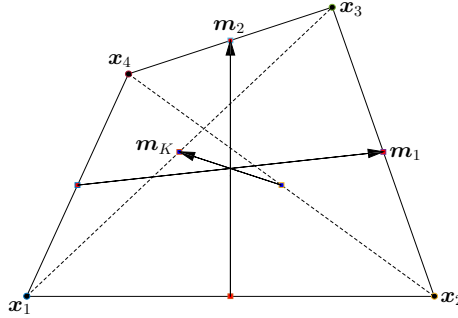


FIGURE 1. Some notations used in the bilinear mapping \mathcal{J}_K .

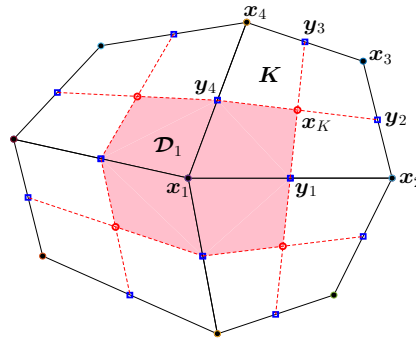


FIGURE 2. The primary mesh \mathcal{T}_h (solid lines) and its associated dual mesh \mathcal{T}_h^* (dotted lines).

where \mathbf{x}_K is the geometric center of K , the vectors \mathbf{m}_1 and \mathbf{m}_2 (resp. \mathbf{m}_K) are related to the midpoints of opposite edges (resp. diagonals) of K , see Figure 1, given by $\mathbf{x}_K = \sum_{i=1}^4 \mathbf{x}_i/4$ and

$$\mathbf{m}_1 = \frac{1}{2}(\mathbf{x}_2 + \mathbf{x}_3 - \mathbf{x}_1 - \mathbf{x}_4), \mathbf{m}_2 = \frac{1}{2}(\mathbf{x}_3 + \mathbf{x}_4 - \mathbf{x}_1 - \mathbf{x}_2), \mathbf{m}_K = \frac{1}{2}(\mathbf{x}_1 + \mathbf{x}_3 - \mathbf{x}_2 - \mathbf{x}_4).$$

Further, we denote \mathcal{C}_h as the set of all geometric centers of \mathcal{T}_h .

On \mathcal{T}_h , the trial function space U_h is defined by

$$U_h = \{u_h \in C(\bar{\Omega}) : u_h|_K = \hat{u}_h \circ \mathcal{J}_K^{-1}, \hat{u}_h|_{\hat{K}} \text{ is bilinear function}, \forall K \in \mathcal{T}_h, u_h|_{\partial\Omega} = 0\}.$$

In each K , by connecting the geometric center \mathbf{x}_K with its four edge midpoints \mathbf{y}_i , we partition K into four quadrilateral sub-elements $\mathcal{D}_{i,K} := \square_{\mathbf{x}_K \mathbf{y}_{i-1} \mathbf{x}_i \mathbf{y}_i}$. Then the whole control volume surrounding \mathbf{x}_i is given by $\mathcal{D}_i = \cup_{K \ni \mathbf{x}_i} \mathcal{D}_{i,K}$, and the dual mesh \mathcal{T}_h^* consists of all control volumes $\mathcal{T}_h^* = \{\mathcal{D}_i : \mathbf{x}_i \in \mathcal{N}_h\}$. That is, all sub-elements sharing a common vertex of the primary mesh form a polygonal element of the dual mesh, see Figure 2 for an example.

On \mathcal{T}_h^* , the test function space V_h is defined as

$$V_h = \text{Span} \{\psi_i : \mathbf{x}_i \in \mathcal{N}_h^\circ\},$$

where ψ_i is the characteristic function satisfying $\psi_i(\mathbf{x}) = 1$ if $\mathbf{x} \in \mathcal{D}_i$, $\psi_i(\mathbf{x}) = 0$ if $\mathbf{x} \in \Omega \setminus \mathcal{D}_i$. It can be checked that $\dim U_h = \dim V_h$.

2.2. The classical Q_1 -FVEM. It follows from (1) and Green’s formula that

$$(5) \quad - \int_{\partial \mathcal{D}_i} (\Lambda \nabla u) \cdot \mathbf{n}_i^* ds = \int_{\mathcal{D}_i} f dx dy, \quad \forall \mathbf{x}_i \in \mathcal{N}_h^\circ,$$

where \mathbf{n}_i^* denotes the unit outward normal vector along the boundary of \mathcal{D}_i . A direct calculation yields that (5) can be rewritten as

$$(6) \quad a_h(u, v_h) = (f, v_h), \quad \forall v_h \in V_h,$$

with

$$a_h(u, v_h) = \sum_{\mathbf{x}_i \in \mathcal{N}_h^\circ} v_i \int_{\partial \mathcal{D}_i} (-\Lambda \nabla u) \cdot \mathbf{n}_i^* ds, \quad (f, v_h) = \sum_{\mathbf{x}_i \in \mathcal{N}_h^\circ} v_i \int_{\mathcal{D}_i} f dx dy$$

and $v_i = v_h(\mathbf{x}_i)$. In (6), replacing u by u_h , which gives the classical Q_1 -FVEM to solve (1) and (2), namely find $u_h \in U_h$ satisfying

$$a_h(u_h, v_h) = (f, v_h), \quad \forall v_h \in V_h.$$

2.3. The Q_1 -FVEM-EM scheme. Noticing $v_i = 0$ if $\mathbf{x}_i \in \partial \Omega$, then by rewriting the bilinear form of $a_h(\cdot, \cdot)$, we have

$$a_h(u_h, v_h) = \sum_{K \in \mathcal{T}_h} a_{K,h}(u_h, v_h),$$

where

$$(7) \quad a_{K,h}(u_h, v_h) = \sum_{i=1}^4 (v_{i+1} - v_i) \int_{\mathbf{x}_K \mathbf{y}_i} (-\Lambda \nabla u_h) \cdot \mathbf{n}_{K,i}^* ds,$$

and

$$\mathbf{n}_{K,i}^* = \frac{1}{\|\mathbf{y}_i - \mathbf{x}_K\|} \mathcal{R}(\mathbf{y}_i - \mathbf{x}_K), \quad \mathcal{R} = \begin{pmatrix} 0 & 1 \\ -1 & 0 \end{pmatrix}.$$

By employing the edge midpoint rule to approximate the line integrals in (7)

$$(8) \quad \int_{\mathbf{x}_K \mathbf{y}_i} (-\Lambda \nabla u_h) \cdot \mathbf{n}_{K,i}^* ds \approx (\mathbf{x}_K - \mathbf{y}_i)^T \mathcal{R}^T \Lambda \nabla u_h(\mathbf{y}_i),$$

then from (8), we obtain the so-called Q_1 -FVEM-EM scheme, given by

$$(9) \quad \tilde{a}_h(u_h, v_h) = (f, v_h), \quad \forall v_h \in V_h,$$

where

$$(10) \quad \tilde{a}_h(u_h, v_h) = \sum_{K \in \mathcal{T}_h} \tilde{a}_{K,h}(u_h, v_h),$$

with

$$(11) \quad \tilde{a}_{K,h}(u_h, v_h) = \sum_{i=1}^4 (v_{i+1} - v_i) (\mathbf{x}_K - \mathbf{y}_i)^T \mathcal{R}^T \Lambda \nabla u_h(\mathbf{y}_i).$$

Remark 1. For the quadrilateral mesh \mathcal{T}_h , let ϕ_i be the isoparametric bilinear nodal basis function at vertex \mathbf{x}_i . Then, we have $u_h = \sum_{j=1}^{nv} u_j \phi_j$, where nv is the number of interior vertices. As a result, (9) can be written as the following linear algebraic system

$$\mathbb{A} \mathbf{u} = \mathbf{b},$$

where

$$\mathbb{A} = (a_{ij})_{nv \times nv}, \quad \mathbf{u} = (u_i)_{nv \times 1}, \quad \mathbf{b} = (b_i)_{nv \times 1},$$

and

$$a_{ij} = \tilde{a}_h(\phi_j, \psi_i), \quad b_i = (f, \psi_i)_{\mathcal{D}_i} = \int_{\mathcal{D}_i} f \, dx dy.$$

We mention that if Λ is the identity matrix, \mathcal{T}_h is square mesh, and the double integral $(f, \psi_i)_{\mathcal{D}_i}$ is computed by approximating at vertex \mathbf{x}_i , then by a straightforward calculation, the Q_1 -FVEM-EM scheme (9) is identical to the standard five-point difference scheme.

3. Stability

3.1. Preliminary. We call \mathcal{T}_h is *regular* (c.f. [36]) provided that there exists a constant C_r independent of K and h , such that

$$(12) \quad \frac{h_K}{\rho_K} \leq C_r, \quad \forall K \in \mathcal{T}_h,$$

where $\rho_K = \min_{1 \leq i \leq 4} \{\text{diameter of circle inscribed in } \Delta \mathbf{x}_{i-1} \mathbf{x}_i \mathbf{x}_{i+1}\}$. Let Π_h^* be a linear mapping which maps $u_h \in U_h$ to $u_h^* := \Pi_h^* u_h \in V_h$ satisfying

$$u_h^*(\mathbf{x}) = u_h(\mathbf{x}), \quad \forall \mathbf{x} \in \mathcal{N}_h^\circ.$$

For the mapping \mathcal{J}_K appeared in (4), we reach its Jacobian matrix as below

$$\mathbb{J}_K(\xi, \eta) = \begin{pmatrix} \frac{\partial x}{\partial \xi} & \frac{\partial y}{\partial \xi} \\ \frac{\partial x}{\partial \eta} & \frac{\partial y}{\partial \eta} \end{pmatrix} = \frac{1}{2} (\mathbf{m}_1 + \mathbf{m}_K \eta, \mathbf{m}_2 + \mathbf{m}_K \xi)^T,$$

where $(x, y)^T = \mathbf{x} = \mathcal{J}_K(\xi, \eta)$. Moreover, the determinant of the Jacobian matrix \mathbb{J}_K is given by

$$\det \mathbb{J}_K(\xi, \eta) = \frac{1}{4} (\mathbf{m}_1 + \mathbf{m}_K \eta) \cdot (\mathcal{R} \mathbf{m}_2 + \mathcal{R} \mathbf{m}_K \xi) = \frac{1}{4} |K| (1 + \bar{\beta}_K \xi + \bar{\gamma}_K \eta),$$

where

$$(13) \quad \bar{\beta}_K = \frac{\mathbf{m}_1 \cdot (\mathcal{R} \mathbf{m}_K)}{|K|} = \frac{S_{123} - S_{412}}{|K|}, \quad \bar{\gamma}_K = \frac{\mathbf{m}_K \cdot (\mathcal{R} \mathbf{m}_2)}{|K|} = \frac{S_{341} - S_{412}}{|K|},$$

$S_{i-1, i, i+1}$ denotes the area of $\Delta \mathbf{x}_{i-1} \mathbf{x}_i \mathbf{x}_{i+1}$ (here $S_{012} = S_{412}$ and $S_{345} = S_{341}$), and we have used the fact $\mathbf{m}_1 \cdot (\mathcal{R} \mathbf{m}_2) = |K|$. Further

$$(14) \quad \mathbb{J}_K^{-1}(\xi, \eta) = \begin{pmatrix} \frac{\partial \xi}{\partial x} & \frac{\partial \eta}{\partial x} \\ \frac{\partial \xi}{\partial y} & \frac{\partial \eta}{\partial y} \end{pmatrix} = \frac{2}{|K| (1 + \bar{\beta}_K \xi + \bar{\gamma}_K \eta)} \mathcal{R}(\mathbf{m}_2 + \xi \mathbf{m}_K, -\mathbf{m}_1 - \eta \mathbf{m}_K).$$

Since

$$\begin{aligned} \widehat{\nabla} \widehat{\phi}_1 &= \frac{1}{4} \begin{pmatrix} \eta - 1 \\ \xi - 1 \end{pmatrix}, & \widehat{\nabla} \widehat{\phi}_2 &= -\frac{1}{4} \begin{pmatrix} \eta - 1 \\ \xi + 1 \end{pmatrix}, \\ \widehat{\nabla} \widehat{\phi}_3 &= \frac{1}{4} \begin{pmatrix} \eta + 1 \\ \xi + 1 \end{pmatrix}, & \widehat{\nabla} \widehat{\phi}_4 &= -\frac{1}{4} \begin{pmatrix} \eta + 1 \\ \xi - 1 \end{pmatrix}, \end{aligned}$$

where $\widehat{\nabla} = (\partial/\partial \xi, \partial/\partial \eta)^T$, thus

$$\mathbb{J}_K^{-1}(\xi, \eta) \widehat{\nabla} \widehat{\phi}_i = \varphi_{i-1} - \varphi_i, \quad i = 1, 2, 3, 4,$$

with

$$(15) \quad \begin{aligned} \varphi_1(\xi, \eta) &= \frac{1}{4} \mathbb{J}_K^{-1}(\xi, \eta) \begin{pmatrix} 1 - \eta \\ 0 \end{pmatrix}, & \varphi_2(\xi, \eta) &= \frac{1}{4} \mathbb{J}_K^{-1}(\xi, \eta) \begin{pmatrix} 0 \\ 1 + \xi \end{pmatrix}, \\ \varphi_3(\xi, \eta) &= -\frac{1}{4} \mathbb{J}_K^{-1}(\xi, \eta) \begin{pmatrix} 1 + \eta \\ 0 \end{pmatrix}, & \varphi_4(\xi, \eta) &= \frac{1}{4} \mathbb{J}_K^{-1}(\xi, \eta) \begin{pmatrix} 0 \\ \xi - 1 \end{pmatrix}. \end{aligned}$$

As a result, for any $u_h \in U_h$, in each K

$$\nabla u_h = \mathbb{J}_K^{-1} \sum_{i=1}^4 u_i \widehat{\nabla} \widehat{\phi}_i = \sum_{i=1}^4 u_i (\varphi_{i-1} - \varphi_i) = \sum_{i=1}^4 (u_{i+1} - u_i) \varphi_i,$$

and it follows from (11) that

$$(16) \quad \widetilde{a}_{K,h}(u_h, u_h^*) = \sum_{i=1}^4 \sum_{j=1}^4 (u_{i+1} - u_i)(u_{j+1} - u_j) (\mathbf{x}_K - \mathbf{y}_i)^T \mathcal{R}^T \Lambda \varphi_j(\widehat{\mathbf{y}}_i) = \delta U_K^T \mathbb{A}_K \delta U_K,$$

where $\widehat{\mathbf{y}}_i = \mathcal{J}_K^{-1}(\mathbf{y}_i)$, $\delta U_K = (u_2 - u_1, u_3 - u_2, u_4 - u_3, u_1 - u_4)^T$ and

$$(17) \quad \mathbb{A}_K = (a_{K,ij})_{4 \times 4}, \quad a_{K,ij} = (\mathbf{x}_K - \mathbf{y}_i)^T \mathcal{R}^T \Lambda \varphi_j(\widehat{\mathbf{y}}_i).$$

3.2. A coercivity result. To present the coercivity result, in each K , we first introduce the following notations

$$(18) \quad m_{ij} = \frac{1}{4|K|} (\mathcal{R} \mathbf{m}_i)^T \Lambda (\mathcal{R} \mathbf{m}_j), \quad \mu_1 = \frac{2m_{11}}{1 - \overline{\beta}_K^2}, \quad \mu_2 = \frac{2m_{22}}{1 - \overline{\gamma}_K^2}, \quad i, j = 1, 2$$

and

$$(19) \quad \zeta_1 = m_{22} - \frac{1}{8} \mu_1 \overline{\gamma}_K^2, \quad \zeta_2 = m_{11} - \frac{1}{8} \mu_2 \overline{\beta}_K^2.$$

Further, we introduce the following assumption.

(A1) There exists a positive constant ϱ , independent of K and h , such that

$$(20) \quad \zeta_1 \zeta_2 - m_{12}^2 \geq \varrho.$$

The meaning of (A1) on some special quadrilateral meshes will be discussed in Section 9 (Appendix B). The main result of this subsection is presented in the following Theorem 1.

Theorem 1. Assume that \mathcal{T}_h is regular, then under the assumption (A1), we have

$$(21) \quad \widetilde{a}_h(u_h, u_h^*) \gtrsim |u_h|_1^2, \quad \forall u_h \in U_h,$$

where the hidden constant independent of K and h , and $|\cdot|_1$ is the standard H^1 semi-norm.

The proof of above Theorem 1 is given at the end of this subsection, here we first give some preliminary lemmas, and some lemmas available in the literature are presented in 8 (Appendix A).

Lemma 1. For the ζ_i ($i = 1, 2$) defined by (19), we have

$$(22) \quad \zeta_1 + \zeta_2 > 0.$$

Proof. By (40), we have $|\bar{\beta}_K| < 1$ and $|\bar{\gamma}_K| < 1$, lead to $\bar{\beta}_K^2 + \bar{\gamma}_K^2 \leq |\bar{\beta}_K| + |\bar{\gamma}_K| < 1$. Thus, it follows from (19) and (18) that

$$\begin{aligned} \zeta_1 + \zeta_2 &= (m_{11} + m_{22}) - \frac{1}{4} \left(\frac{\bar{\gamma}_K^2}{1 - \bar{\beta}_K^2} m_{11} + \frac{\bar{\beta}_K^2}{1 - \bar{\gamma}_K^2} m_{22} \right) \\ &> (m_{11} + m_{22}) - \frac{1}{4} (m_{11} + m_{22}) = \frac{3}{4} (m_{11} + m_{22}) > 0. \end{aligned}$$

□

Lemma 2. For the φ_i defined by (15), we have

$$\begin{aligned} \varphi_i(\widehat{\mathbf{y}}_{i+2}) &= \mathbf{0}, \quad i = 1, 2, 3, 4, \\ \varphi_1(\widehat{\mathbf{y}}_1) &= \frac{1}{(1 - \bar{\gamma}_K) |K|} \mathcal{R}m_2, \quad \varphi_2(\widehat{\mathbf{y}}_2) = -\frac{1}{(1 + \bar{\beta}_K) |K|} \mathcal{R}m_1, \\ \varphi_3(\widehat{\mathbf{y}}_3) &= -\frac{1}{(1 + \bar{\gamma}_K) |K|} \mathcal{R}m_2, \quad \varphi_4(\widehat{\mathbf{y}}_4) = \frac{1}{(1 - \bar{\beta}_K) |K|} \mathcal{R}m_1, \\ (23) \quad \varphi_1(\widehat{\mathbf{y}}_2) &= -\varphi_3(\widehat{\mathbf{y}}_2) = \frac{\bar{\gamma}_K}{2(1 + \bar{\beta}_K) |K|} \mathcal{R}m_1 + \frac{1}{2|K|} \mathcal{R}m_2, \\ \varphi_1(\widehat{\mathbf{y}}_4) &= -\varphi_3(\widehat{\mathbf{y}}_4) = -\frac{\bar{\gamma}_K}{2(1 - \bar{\beta}_K) |K|} \mathcal{R}m_1 + \frac{1}{2|K|} \mathcal{R}m_2, \\ \varphi_2(\widehat{\mathbf{y}}_1) &= -\varphi_4(\widehat{\mathbf{y}}_1) = -\frac{1}{2|K|} \mathcal{R}m_1 + \frac{\bar{\beta}_K}{2(1 - \bar{\gamma}_K) |K|} \mathcal{R}m_2, \\ \varphi_2(\widehat{\mathbf{y}}_3) &= -\varphi_4(\widehat{\mathbf{y}}_3) = -\frac{1}{2|K|} \mathcal{R}m_1 - \frac{\bar{\beta}_K}{2(1 + \bar{\gamma}_K) |K|} \mathcal{R}m_2. \end{aligned}$$

Proof. It follows from (14) and (15) that

$$\varphi_i(\widehat{\mathbf{y}}_{i+2}) = \mathbb{J}_K^{-1}(\widehat{\mathbf{y}}_{i+2}) \mathbf{0} = \mathbf{0}$$

and

$$\varphi_1(\widehat{\mathbf{y}}_1) = \frac{1}{4} \mathbb{J}_K^{-1}(0, -1) \begin{pmatrix} 2 \\ 0 \end{pmatrix} = \frac{1}{(1 - \bar{\gamma}_K) |K|} \mathcal{R}m_2.$$

Noticing (39), we can obtain the rest identities in (23) by the same arguments. □

Lemma 3. For the \mathbb{A}_K defined by (17), we have

$$\mathbb{A}_K = \begin{pmatrix} \frac{2}{1 - \bar{\gamma}_K} m_{22} & \frac{\bar{\beta}_K}{1 - \bar{\gamma}_K} m_{22} - m_{12} & 0 & m_{12} - \frac{\bar{\beta}_K}{1 - \bar{\gamma}_K} m_{22} \\ -\frac{\bar{\gamma}_K}{1 + \bar{\beta}_K} m_{11} - m_{12} & \frac{2}{1 + \bar{\beta}_K} m_{11} & \frac{\bar{\gamma}_K}{1 + \bar{\beta}_K} m_{11} + m_{12} & 0 \\ 0 & m_{12} + \frac{\bar{\beta}_K}{1 + \bar{\gamma}_K} m_{22} & \frac{2}{1 + \bar{\gamma}_K} m_{22} & -m_{12} - \frac{\bar{\beta}_K}{1 + \bar{\gamma}_K} m_{22} \\ m_{12} - \frac{\bar{\gamma}_K}{1 - \bar{\beta}_K} m_{11} & 0 & \frac{\bar{\gamma}_K}{1 - \bar{\beta}_K} m_{11} - m_{12} & \frac{2}{1 - \bar{\beta}_K} m_{11} \end{pmatrix}.$$

Proof. Note that

$$\mathbf{x}_K - \mathbf{y}_1 = \mathbf{y}_3 - \mathbf{x}_K = \frac{1}{2} \mathbf{m}_2, \quad \mathbf{x}_K - \mathbf{y}_4 = \mathbf{y}_2 - \mathbf{x}_K = \frac{1}{2} \mathbf{m}_1,$$

then by (17), (23), (18) and some straightforward calculations, we can obtain each entry of \mathbb{A}_K and complete the proof. □

Assume that

$$(24) \quad \mathbb{B}_K = \frac{1}{2} (\mathbb{A}_K + \mathbb{A}_K^T)$$

is the symmetric part of \mathbb{A}_K , and

$$(25) \quad \mathbb{T} = \mathbb{T}_1 \mathbb{T}_2 \mathbb{T}_3$$

with

$$\mathbb{T}_1 = \begin{pmatrix} 1 & 0 & 0 & 0 \\ 0 & 0 & 1 & 0 \\ 0 & -1 & 0 & 0 \\ 0 & 0 & 0 & -1 \end{pmatrix}, \quad \mathbb{T}_3 = \begin{pmatrix} 1 & 0 & -\frac{\bar{\beta}_K}{4} & 0 \\ 0 & 1 & 0 & 0 \\ 0 & 0 & 1 & 0 \\ 0 & -\frac{\bar{\gamma}_K}{4} & 0 & 1 \end{pmatrix},$$

$$\mathbb{T}_2 = \begin{pmatrix} \mathbb{T}_{21} & \mathbb{O} \\ \mathbb{O} & \mathbb{T}_{22} \end{pmatrix}, \quad \mathbb{T}_{21} = \begin{pmatrix} 1 & \frac{1 - \bar{\gamma}_K}{2} \\ -1 & \frac{1 + \bar{\gamma}_K}{2} \end{pmatrix}, \quad \mathbb{T}_{22} = \begin{pmatrix} \frac{1 + \bar{\beta}_K}{2} & -1 \\ \frac{1 - \bar{\beta}_K}{2} & 1 \end{pmatrix},$$

and \mathbb{O} is a 2×2 matrix with all entries equal to zero.

Lemma 4. *For the \mathbb{B}_K defined by (24), we have*

$$(26) \quad \mathbb{T}^T \mathbb{B}_K \mathbb{T} = \begin{pmatrix} 2\mu_2 & 0 & 0 & 0 \\ 0 & \zeta_1 & -m_{12} & 0 \\ 0 & -m_{12} & \zeta_2 & 0 \\ 0 & 0 & 0 & 2\mu_1 \end{pmatrix}.$$

Consequently, \mathbb{B}_K is a positive definite matrix if and only if

$$(27) \quad \zeta_1 \zeta_2 - m_{12}^2 > 0.$$

Proof. By the definition of \mathbb{T}_1 , we deduce that

$$\mathbb{T}_1^T \mathbb{B}_K \mathbb{T}_1 = \begin{pmatrix} \mathbb{B}_{11} & \mathbb{B}_{13} \\ \mathbb{B}_{13}^T & \mathbb{B}_{12} \end{pmatrix},$$

where

$$\mathbb{B}_{11} = \begin{pmatrix} \frac{2}{1 - \bar{\gamma}_K} m_{22} & 0 \\ 0 & \frac{2}{1 + \bar{\gamma}_K} m_{22} \end{pmatrix}, \quad \mathbb{B}_{12} = \begin{pmatrix} \frac{2}{1 + \bar{\beta}_K} m_{11} & 0 \\ 0 & \frac{2}{1 - \bar{\beta}_K} m_{11} \end{pmatrix},$$

$$\mathbb{B}_{13} = \begin{pmatrix} -\frac{\bar{\gamma}_K}{2(1 + \bar{\beta}_K)} m_{11} - m_{12} + \frac{\bar{\beta}_K}{2(1 - \bar{\gamma}_K)} m_{22} & \frac{\bar{\gamma}_K}{2(1 - \bar{\beta}_K)} m_{11} - m_{12} + \frac{\bar{\beta}_K}{2(1 - \bar{\gamma}_K)} m_{22} \\ -\frac{\bar{\gamma}_K}{2(1 + \bar{\beta}_K)} m_{11} - m_{12} - \frac{\bar{\beta}_K}{2(1 + \bar{\gamma}_K)} m_{22} & \frac{\bar{\gamma}_K}{2(1 - \bar{\beta}_K)} m_{11} - m_{12} - \frac{\bar{\beta}_K}{2(1 + \bar{\gamma}_K)} m_{22} \end{pmatrix}.$$

By some direct but tedious calculations, we have

$$\mathbb{T}_{21}^T \mathbb{B}_{11} \mathbb{T}_{21} = \begin{pmatrix} 2\mu_2 & 0 \\ 0 & m_{22} \end{pmatrix}, \quad \mathbb{T}_{22}^T \mathbb{B}_{12} \mathbb{T}_{22} = \begin{pmatrix} m_{11} & 0 \\ 0 & 2\mu_1 \end{pmatrix},$$

$$\mathbb{T}_{21}^T \mathbb{B}_{13} \mathbb{T}_{22} = \begin{pmatrix} \frac{1}{2} \bar{\beta}_K \mu_2 & 0 \\ -m_{12} & \frac{1}{2} \bar{\gamma}_K \mu_1 \end{pmatrix},$$

where μ_i is defined in (18). It follows that

$$\mathbb{T}_2^T \mathbb{T}_1^T \mathbb{B}_K \mathbb{T}_1 \mathbb{T}_2 = \begin{pmatrix} 2\mu_2 & 0 & \frac{1}{2}\bar{\beta}_K \mu_2 & 0 \\ 0 & m_{22} & -m_{12} & \frac{1}{2}\bar{\gamma}_K \mu_1 \\ \frac{1}{2}\bar{\beta}_K \mu_2 & -m_{12} & m_{11} & 0 \\ 0 & \frac{1}{2}\bar{\gamma}_K \mu_1 & 0 & 2\mu_1 \end{pmatrix}.$$

As a result, still by some direct calculations with \mathbb{T}_3 , we obtain (26). Note that \mathbb{T}_i ($i = 1, 2, 3$) are all invertible matrices and $\mu_i > 0$ ($i = 1, 2$), thus we find that \mathbb{B}_K is a positive definite matrix if and only if the two roots of characteristic equation

$$(28) \quad \lambda^2 - (\zeta_1 + \zeta_2)\lambda + \zeta_1\zeta_2 - m_{12}^2 = 0$$

are all positive. Recalling (22), then the two roots of (28) are all positive, is equivalent to (27). The proof is complete. \square

Lemma 5. *Assume that \mathcal{T}_h is regular and (A1) holds, then \mathbb{B}_K is uniformly positive definite matrix and satisfying*

$$(29) \quad \mathbf{v}^T \mathbb{B}_K \mathbf{v} \geq \frac{64\pi\rho}{289\lambda C_r} \|\mathbf{v}\|^2, \quad \forall \mathbf{v} \in \mathbb{R}^4.$$

Proof. It follows from (26) that

$$\mathbf{v}^T \mathbb{B}_K \mathbf{v} = (\mathbb{T}^{-1}\mathbf{v})^T (\mathbb{T}^T \mathbb{B}_K \mathbb{T}) (\mathbb{T}^{-1}\mathbf{v}) \geq \lambda_K \|\mathbb{T}^{-1}\mathbf{v}\|^2,$$

where $\lambda_K = \min\{2\mu_1, 2\mu_2, \lambda'_K\}$ and λ'_K is the minimum root of characteristic equation (28), given by

$$\lambda'_K = \frac{1}{2} \left[\zeta_1 + \zeta_2 - \sqrt{(\zeta_1 + \zeta_2)^2 - 4(\zeta_1\zeta_2 - m_{12}^2)} \right].$$

By (18) and (40), we have $2\mu_1 \geq 4m_{11}$ and $2\mu_2 \geq 4m_{22}$. Since (A1) holds, then from (19) and (20)

$$\lambda'_K = \frac{2(\zeta_1\zeta_2 - m_{12}^2)}{\zeta_1 + \zeta_2 + \sqrt{(\zeta_1 + \zeta_2)^2 - 4(\zeta_1\zeta_2 - m_{12}^2)}} > \frac{\zeta_1\zeta_2 - m_{12}^2}{\zeta_1 + \zeta_2} \geq \frac{\zeta_1\zeta_2 - m_{12}^2}{m_{11} + m_{22}}.$$

Since \mathcal{T}_h is regular, then (42) holds, and we obtain

$$\lambda_K \geq \min \left\{ 4m_{11}, 4m_{22}, \frac{\zeta_1\zeta_2 - m_{12}^2}{m_{11} + m_{22}} \right\} = \frac{\zeta_1\zeta_2 - m_{12}^2}{m_{11} + m_{22}} > \frac{\pi\rho}{\lambda C_r},$$

where we have used the fact

$$\frac{\zeta_1\zeta_2 - m_{12}^2}{m_{11} + m_{22}} \leq \frac{\zeta_1\zeta_2}{m_{11} + m_{22}} \leq \frac{m_{11}m_{22}}{m_{11} + m_{22}} < \min\{m_{11}, m_{22}\}.$$

Moreover, we deduce from (43) that

$$\|\mathbb{T}^{-1}\mathbf{v}\| \geq \frac{1}{\|\mathbb{T}\|} \|\mathbf{v}\| \geq \frac{8}{17} \|\mathbf{v}\|.$$

Therefore, the desired result (29) follows immediately. \square

The proof of Theorem 1. It follows from (10), (16), (24), (29) and (44) that

$$\tilde{a}_h(u_h, u_h^*) = \sum_{K \in \mathcal{T}_h} \delta U_K^T \mathbb{B}_K \delta U_K \geq \frac{64\pi\rho}{289\lambda C_r} \sum_{K \in \mathcal{T}_h} \|\delta U_K\|^2 \geq \frac{64\pi\rho}{289\lambda C_r C^2} |u_h|_1^2,$$

which leads to (21) and completes the proof of Theorem 1. \square

3.3. A stability result.

Theorem 2. Let u_h be the finite volume element solution of (9). Then, under the assumptions (12) and (A1), we have

$$(30) \quad |u_h|_1 \lesssim \|f\|_0.$$

Proof. It follows from (21) and (9) that

$$|u_h|_1^2 \lesssim \tilde{a}_h(u_h, u_h^*) = (f, u_h^*) \leq \|f\|_0 \|u_h^*\|_0.$$

A direct calculation yields that

$$\|u_h\|_{0,K}^2 = \int_{\hat{K}} \hat{u}_h^2 \det \mathbb{J}_K(\xi, \eta) \, d\xi d\eta \gtrsim h_K^2 \|\hat{u}_h\|_{0,\hat{K}}^2,$$

where we have used the fact $\det \mathbb{J}_K(\xi, \eta)$ is a linear function on \hat{K} and

$$\begin{aligned} \det \mathbb{J}_K(\xi, \eta) &\geq \min_{1 \leq i \leq 4} \det \mathbb{J}_K(\hat{\mathbf{x}}_i) \\ &= \frac{1}{4} |K| \min \{1 - \bar{\beta}_K - \bar{\gamma}_K, 1 + \bar{\beta}_K - \bar{\gamma}_K, 1 + \bar{\beta}_K + \bar{\gamma}_K, 1 - \bar{\beta}_K + \bar{\gamma}_K\} \\ &= \frac{1}{2} \min \{S_{412}, S_{123}, S_{234}, S_{341}\} \\ &> \frac{1}{2} \pi \left(\frac{\rho_K}{2}\right)^2 \geq \frac{\pi}{8C_r^2} h_K^2, \quad \forall (\xi, \eta) \in \hat{K}. \end{aligned}$$

Note that $\|\hat{u}_h\|_{0,\hat{K}}^2$ and $\sum_{i=1}^4 u_i^2$ are two equivalent norms on \hat{K} , we obtain

$$\begin{aligned} \|u_h^*\|_0^2 &= \sum_{K \in \mathcal{T}_h} \|u_h^*\|_{0,K}^2 \leq \sum_{K \in \mathcal{T}_h} \left(h_K^2 \sum_{i=1}^4 u_i^2 \right) \lesssim \sum_{K \in \mathcal{T}_h} \left(h_K^2 \|\hat{u}_h\|_{0,\hat{K}}^2 \right) \\ &\lesssim \sum_{K \in \mathcal{T}_h} \|u_h\|_{0,K}^2 = \|u_h\|_0^2 \lesssim |u_h|_1^2, \end{aligned}$$

where in the last inequality we have used the Poincaré inequality. Combining the above results, we reach (30). \square

4. Superconvergence

4.1. Preliminary. \mathcal{T}_h is called h^2 -uniform mesh (c.f. [37, 31]) if the inequality (47) holds for each $K \in \mathcal{T}_h$, and for arbitrary two adjacent quadrilateral elements $K_1 = \square \mathbf{x}_1 \mathbf{x}_2 \mathbf{x}_3 \mathbf{x}_4$ and $K_2 = \square \mathbf{x}_4 \mathbf{x}_3 \mathbf{x}_5 \mathbf{x}_6$ of \mathcal{T}_h (see Figure 3), there exists a constant $C > 0$ such that there holds the following h^2 -parallelogram condition

$$\|(\mathbf{x}_4 - \mathbf{x}_1) + (\mathbf{x}_4 - \mathbf{x}_6)\| \leq Ch^2.$$

If \mathcal{T}_h is h^2 -uniform, we have

$$(31) \quad \|2\mathbf{y}_3 - \mathbf{x}_{K_1} - \mathbf{x}_{K_2}\| \lesssim h^2.$$

Suppose that $u_I \in U_h$ is the isoparametric bilinear interpolation of u satisfying $u_I(\mathbf{x}_i) = u(\mathbf{x}_i)$, $\forall \mathbf{x}_i \in \mathcal{N}_h$, where \mathcal{N}_h denotes the set of all vertices of \mathcal{T}_h .

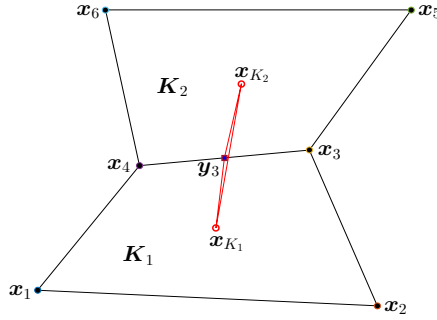


FIGURE 3. Some notations used to define the h^2 -uniform mesh.

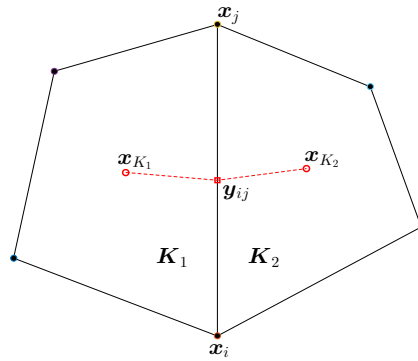


FIGURE 4. Some notations used in Lemmas 6 and 7.

4.2. A superconvergence result. By (21)

$$(32) \quad |u_I - u_h|_1^2 \lesssim \tilde{a}_h(u_I - u_h, (u_I - u_h)^*) = E_1 + E_2,$$

where

$$E_1 = \tilde{a}_h(u_I - u, (u_I - u_h)^*), \quad E_2 = \tilde{a}_h(u - u_h, (u_I - u_h)^*).$$

In the following discussions, we will estimate E_1 and E_2 respectively.

Lemma 6. Assume that $u \in H_0^1(\Omega) \cap W^{3,\infty}(\Omega)$ is the exact solution of (1) and (2), $u_h \in U_h$ is the Q_1 -finite volume element solution of (9). Then, if \mathcal{T}_h is h^2 -uniform, we have

$$(33) \quad |E_1| \lesssim h^2 \|u\|_{3,\infty} |u_I - u_h|_{1,\Omega,h},$$

where

$$|u_I - u_h|_{1,\Omega,h}^2 = \sum_{K \in \mathcal{T}_h} |u_I - u_h|_{1,K,h}^2.$$

Proof. For arbitrary two adjacent quadrilateral elements $K_1, K_2 \in \mathcal{T}_h$, we denote its common edge as $\mathbf{x}_i \mathbf{x}_j \in \mathcal{E}_h^\circ$, see Figure 4, and assume that the midpoint of $\mathbf{x}_i \mathbf{x}_j$ is \mathbf{y}_{ij} . Since \mathcal{T}_h is h^2 -uniform, then by (31)

$$(34) \quad \|2\mathbf{y}_{ij} - \mathbf{x}_{K_1} - \mathbf{x}_{K_2}\| \lesssim h^2.$$

Recalling $(u_I - u_h)^* = 0$ on $\partial\Omega$ and the number of elements in \mathcal{T}_h is $\mathcal{O}(h^{-2})$, then we deduce from (10), (11) and (45) that

$$\begin{aligned}
|E_1| &= \left| \sum_{K \in \mathcal{T}_h} \tilde{a}_{K,h}(u - u_I, (u_I - u_h)^*) \right| \\
&= \left| \sum_{\mathbf{x}_i \mathbf{x}_j \in \mathcal{E}_h^\circ} [(u_I - u_h)^*]_{\mathbf{x}_{K_1} \mathbf{x}_{K_2}} \left((\mathbf{x}_{K_1} - \mathbf{y}_{ij})^T \mathcal{R}^T \Lambda \nabla_{K_1}(u - u_I)(\mathbf{y}_{ij}) \right. \right. \\
&\quad \left. \left. + (\mathbf{y}_{ij} - \mathbf{x}_{K_2})^T \mathcal{R}^T \Lambda \nabla_{K_2}(u - u_I)(\mathbf{y}_{ij}) \right) \right| \\
&= \left| \sum_{\mathbf{x}_i \mathbf{x}_j \in \mathcal{E}_h^\circ} [(u_I - u_h)^*]_{\mathbf{x}_{K_1} \mathbf{x}_{K_2}} \left(2(\mathbf{x}_{K_1} - \mathbf{y}_{ij})^T \mathcal{R}^T \Lambda \bar{\nabla}(u - u_I)(\mathbf{y}_{ij}) \right. \right. \\
&\quad \left. \left. + (2\mathbf{y}_{ij} - \mathbf{x}_{K_1} - \mathbf{x}_{K_2})^T \mathcal{R}^T \Lambda \nabla_{K_2}(u - u_I)(\mathbf{y}_{ij}) \right) \right| \\
&\lesssim \sum_{\mathbf{x}_i \mathbf{x}_j \in \mathcal{E}_h^\circ} |u_I - u_h|_{1, K_1, h} [h \|\bar{\nabla}(u - u_I)(\mathbf{y}_{ij})\| + h^2 \|\nabla_{K_2}(u - u_I)(\mathbf{y}_{ij})\|] \\
&\lesssim h^3 \|u\|_{3, \infty} \sum_{\mathbf{x}_i \mathbf{x}_j \in \mathcal{E}_h^\circ} |u_I - u_h|_{1, K_1, h} \\
&\lesssim h^2 \|u\|_{3, \infty} |u_I - u_h|_{1, \Omega, h},
\end{aligned}$$

where ∇_{K_i} denotes the gradient ∇ that restrict on K_i , $i = 1, 2$,

$$[(u_I - u_h)^*]_{\mathbf{x}_{K_1} \mathbf{x}_{K_2}} = (u_I - u_h)(\mathbf{x}_j) - (u_I - u_h)(\mathbf{x}_i),$$

and the fact

$$\|\nabla_{K_2}(u - u_I)(\mathbf{y}_{ij})\| \lesssim h \|u\|_{3, \infty}$$

is used, which can be proved by Taylor's expansion, the proof is similar to that of Theorem 1 in [38]. Thus, the desired result (33) is verified. \square

Lemma 7. *Let $u \in H_0^1(\Omega) \cap W^{3, \infty}(\Omega)$ be the exact solution of (1) and (2), $u_h \in U_h$ the Q_1 -finite volume element solution of (9). Moreover, we assume that \mathcal{T}_h is h^2 -uniform. Then, we have*

$$(35) \quad |E_2| \lesssim h^2 \|u\|_{3, \infty} |u_I - u_h|_{1, \Omega, h}.$$

Proof. It follows from (6) and (9) that

$$a_h(u, v_h) = (f, v_h) = \tilde{a}_h(u_h, v_h), \quad \forall v_h \in V_h.$$

Then, we have

$$|E_2| = |\tilde{a}_h(u, (u_I - u_h)^*) - a_h(u, (u_I - u_h)^*)| = |E_{21} + E_{22}|,$$

where

$$\begin{aligned} |E_{21}| &= \left| \sum_{K \in \mathcal{T}_h} \sum_{i=1}^4 [(u_I - u_h)^*]_{\mathbf{x}_K \mathbf{y}_i} \left(\int_{\mathbf{x}_K \mathbf{y}_i} (-\Lambda \nabla u) \cdot \mathbf{n}_{K,i}^* \, ds \right. \right. \\ &\quad \left. \left. - \frac{1}{2} (\mathbf{x}_K - \mathbf{y}_i)^T \mathcal{R}^T \Lambda (\nabla u(\mathbf{x}_K) + \nabla u(\mathbf{y}_i)) \right) \right| \\ &\lesssim \sum_{K \in \mathcal{T}_h} \sum_{i=1}^4 h_K^3 |u_I - u_h|_{1,K,h} \|u\|_{3,\infty,K} \lesssim h^3 \|u\|_{3,\infty} \sum_{K \in \mathcal{T}_h} |u_I - u_h|_{1,K,h} \\ &\lesssim h^2 \|u\|_{3,\infty} |u_I - u_h|_{1,\Omega,h}, \end{aligned}$$

in the above inequality we have used the quadrature error of trapezoidal rule and the number of elements in \mathcal{T}_h is $\mathcal{O}(h^{-2})$,

$$[(u_I - u_h)^*]_{\mathbf{x}_K \mathbf{y}_i} = (u_I - u_h)(\mathbf{x}_{i+1}) - (u_I - u_h)(\mathbf{x}_i)$$

and (cf. Figure 4)

$$\begin{aligned} |E_{22}| &= \left| \sum_{K \in \mathcal{T}_h} \sum_{i=1}^4 [(u_I - u_h)^*]_{\mathbf{x}_K \mathbf{y}_i} \frac{1}{2} \left((\mathbf{x}_K - \mathbf{y}_i)^T \mathcal{R}^T \Lambda (\nabla u(\mathbf{x}_K) - \nabla u(\mathbf{y}_i)) \right) \right| \\ &= \frac{1}{2} \left| \sum_{\mathbf{x}_i \mathbf{x}_j \in \mathcal{E}_h^\circ} [(u_I - u_h)^*]_{\mathbf{x}_{K_1} \mathbf{x}_{K_2}} F_{K_1, K_2} \right|, \end{aligned}$$

with

$$\begin{aligned} F_{K_1, K_2} &= (\mathbf{x}_{K_1} - \mathbf{y}_{ij})^T \mathcal{R}^T \Lambda (\nabla_{K_1} u(\mathbf{x}_{K_1}) - \nabla_{K_1} u(\mathbf{y}_{ij})) \\ &\quad - (\mathbf{x}_{K_2} - \mathbf{y}_{ij})^T \mathcal{R}^T \Lambda (\nabla_{K_2} u(\mathbf{x}_{K_2}) - \nabla_{K_2} u(\mathbf{y}_{ij})). \end{aligned}$$

By Taylor's expansion and (34)

$$\begin{aligned} |F_{K_1, K_2}| &= |(\mathbf{x}_{K_1} - \mathbf{y}_{ij})^T \mathcal{R}^T \Lambda \mathbb{F}(\mathbf{x}_{K_1} - \mathbf{y}_{ij}) - (\mathbf{x}_{K_2} - \mathbf{y}_{ij})^T \mathcal{R}^T \Lambda \mathbb{F}(\mathbf{x}_{K_2} - \mathbf{y}_{ij}) \\ &\quad + \mathcal{O}(h^3) \|u\|_{3,\infty}| \\ &\lesssim h^3 \|u\|_{3,\infty}, \end{aligned}$$

where

$$\mathbb{F} = \begin{pmatrix} \frac{\partial^2 u}{\partial x^2}(\mathbf{y}_{ij}) & \frac{\partial^2 u}{\partial x \partial y}(\mathbf{y}_{ij}) \\ \frac{\partial^2 u}{\partial x \partial y}(\mathbf{y}_{ij}) & \frac{\partial^2 u}{\partial y^2}(\mathbf{y}_{ij}) \end{pmatrix}.$$

It follows that

$$|E_{22}| \lesssim h^3 \|u\|_{3,\infty} \sum_{\mathbf{x}_i \mathbf{x}_j \in \mathcal{E}_h^\circ} |u_I - u_h|_{1,K_1,h} \lesssim h^2 \|u\|_{3,\infty} |u_I - u_h|_{1,\Omega,h}.$$

Combining the above results, we reach (35). □

Theorem 3. *Let $u \in H_0^1(\Omega) \cap W^{3,\infty}(\Omega)$ be the exact solution of (1) and (2), $u_h \in U_h$ the Q_1 -finite volume element solution of (9). Moreover, we assume that \mathcal{T}_h is regular and h^2 -uniform. Then, we have*

$$(36) \quad |u_I - u_h|_1 \lesssim h^2 \|u\|_{3,\infty}.$$

Proof. From (32), (33), (35) and (44), we find that

$$|u_I - u_h|_1^2 \lesssim h^2 \|u\|_{3,\infty} |u_I - u_h|_{1,\Omega,h} \lesssim h^2 \|u\|_{3,\infty} |u_I - u_h|_1.$$

The desired result (36) is proved. □

4.3. Some corollaries.

Corollary 1. *Under the same assumptions to Theorem 3, we have*

$$|u - u_h|_1 \lesssim h \|u\|_{3,\infty}$$

and

$$(37) \quad \|u - u_h\|_0 \lesssim h^2 \|u\|_{3,\infty}.$$

Proof. By the triangle inequality, standard interpolation error estimate and (36), we obtain

$$|u - u_h|_1 \leq |u - u_I|_1 + |u_I - u_h|_1 \lesssim h \|u\|_{3,\infty},$$

and we deduce from Poincaré-Friedrichs inequality that

$$\|u - u_h\|_0 \leq \|u - u_I\|_0 + \|u_I - u_h\|_0 \lesssim \|u - u_I\|_0 + |u_I - u_h|_1 \lesssim h^2 \|u\|_{3,\infty}.$$

□

Remark 2. *The optimal L^2 error estimate (37) is a direct consequence of the superconvergence result (36), and here we do not use the Aubin-Nitsche technique.*

Corollary 2. *Under the same assumptions to Theorem 3, we have*

$$(38) \quad \left(\frac{1}{\#S} \sum_{\mathbf{x} \in S} \|\bar{\nabla}(u - u_h)(\mathbf{x})\|^2 \right)^{\frac{1}{2}} \lesssim h^2 \|u\|_{3,\infty},$$

where S is the set \mathcal{C}_h or \mathcal{N}_h° or \mathcal{M}_h° , and $\#S$ is the cardinality of S .

Proof. By (45)

$$\left(\frac{1}{\#S} \sum_{\mathbf{x} \in S} \|\bar{\nabla}(u - u_I)(\mathbf{x})\|^2 \right)^{\frac{1}{2}} \lesssim h^2 \|u\|_{3,\infty} \left(\frac{1}{\#S} \sum_{\mathbf{x} \in S} 1 \right)^{\frac{1}{2}} \lesssim h^2 \|u\|_{3,\infty}.$$

From the inverse inequality, the fact $\#S = \mathcal{O}(h^{-2})$ and (36), we get

$$\begin{aligned} \left(\frac{1}{\#S} \sum_{\mathbf{x} \in S} \|\bar{\nabla}(u_I - u_h)(\mathbf{x})\|^2 \right)^{\frac{1}{2}} &\lesssim \left(\frac{1}{\#S} \sum_{\mathbf{x} \in S} h^{-2} \|u_I - u_h\|_{1,K_{\mathbf{x}}}^2 \right)^{\frac{1}{2}} \\ &\lesssim \left(\sum_{\mathbf{x} \in S} \|u_I - u_h\|_{1,K_{\mathbf{x}}}^2 \right)^{\frac{1}{2}} \\ &\lesssim \|u_I - u_h\|_1 \lesssim h^2 \|u\|_{3,\infty}, \end{aligned}$$

where $K_{\mathbf{x}} = \cup_{K' \ni \mathbf{x}} \{K'\}$ is the union of quadrilateral element K' that contains \mathbf{x} . Combining the above results, we reach (38). □

5. Numerical experiments

In this section, we present four numerical examples to validate the theoretical findings, and employ four kinds of quadrilateral meshes. The first type (Mesh I) is uniform rectangular mesh, see Figure 5(a), where the coordinates of vertices are as follows

$$h(i - 1, j - 1)^T, \quad 1 \leq i, j \leq n + 1,$$

with $h = 1/n$ is the mesh size. The second one (Mesh II) is a quadrilateral mesh constructed by disturbing the vertices of Mesh I and keeping the connections unchanged, see Figure 5(b), where the coordinates of vertices are given by

$$x_{ij} = (i-1)h, \quad y_{ij} = (j-1)h + \frac{1}{20} \sin(2\pi h(i-1)) \sin(2\pi h(j-1)), \quad 1 \leq i, j \leq n+1.$$

Mesh IV is a uniform trapezoidal mesh also obtained by disturbing some vertices of Mesh I, see Figure 5(d), where the disturbance of a vertex is $h/4$ along y direction. In our numerical experiments, we set $\Omega = (0, 1)^2$ for the Meshes I, II and IV. The third mesh (Mesh III) is a refined one where the initial region Ω_0 is a quadrilateral (see Figure 5(c)), and four coordinates of Ω_0 are given as follows

$$(0, 0)^T, \quad (1, 0)^T, \quad (0.7, 1)^T, \quad (0, 0.8)^T.$$

In other words, Mesh III is constructed by the standard bisection procedure (connecting the midpoints of opposite edges of each quadrilateral), see the thin line segments of Figure 5(c). A direct calculation yields that Meshes I, II and III are all h^2 -uniform. For simplicity of exposition, we define

$$E_C = \left(\frac{1}{\#\mathcal{C}_h} \sum_{\mathbf{x} \in \mathcal{C}_h} \|\bar{\nabla}(u - u_h)(\mathbf{x})\|^2 \right)^{\frac{1}{2}}, \quad E_V = \left(\frac{1}{\#\mathcal{N}_h^\circ} \sum_{\mathbf{x} \in \mathcal{N}_h^\circ} \|\bar{\nabla}(u - u_h)(\mathbf{x})\|^2 \right)^{\frac{1}{2}}$$

and

$$E_{\mathcal{M}} = \left(\frac{1}{\#\mathcal{M}_h^\circ} \sum_{\mathbf{x} \in \mathcal{M}_h^\circ} \|\bar{\nabla}(u - u_h)(\mathbf{x})\|^2 \right)^{\frac{1}{2}}$$

as the errors at geometric centers, interior vertices and edge midpoints respectively. Moreover, note that the assumption **(A1)** is a basis in our theoretical analysis, we denote

$$\varrho = \min_{K \in \mathcal{T}_h} \{\zeta_1 \zeta_2 - m_{12}^2\}.$$

Example 1. Consider the problem (1) and (2), where the anisotropic diffusion tensor and source term are given by

$$\Lambda = \begin{pmatrix} 1 & 2 \\ 2 & 5 \end{pmatrix}, \quad f(x, y) = -10e^{x+y}.$$

This problem allows the following exact solution $u(x, y) = e^{x+y}$.

In Tables 1 and 2, we present the numerical results, ‘‘Order’’ indicates the numerical convergence order computed by $\log_2(E_{2h}/E_h)$, where E_{2h} and E_h are the errors of the corresponding two successive mesh size \mathcal{T}_{2h} and \mathcal{T}_h . We find that for the four meshes and diffusion coefficient, **(A1)** is satisfied. Moreover, for the Meshes I, II and III, the finite volume element solution u_h converges to the interpolation u_I of u with second order under H^1 norm, which validates the superconvergence result in Theorem 3, the rest results in these two tables also confirm the theoretical results in Corollaries 1 and 2. However, for Mesh IV, one can see from Table 2 that, the finite volume element solution does not own the superconvergence, since Mesh IV is not h^2 -uniform. Fortunately, it preserves the optimal convergence orders 1 and 2 under H^1 and L^2 norms.

Example 2. Solve the problem (1) and (2), where the discontinuous anisotropic diffusion tensor is given by

$$\Lambda(x, y) = \begin{cases} \begin{pmatrix} 1.75 & 0.5 \\ 0.5 & 1.75 \end{pmatrix}, & x \leq 0.5, \\ \begin{pmatrix} 3 & 1 \\ 1 & 2 \end{pmatrix}, & x > 0.5. \end{cases}$$

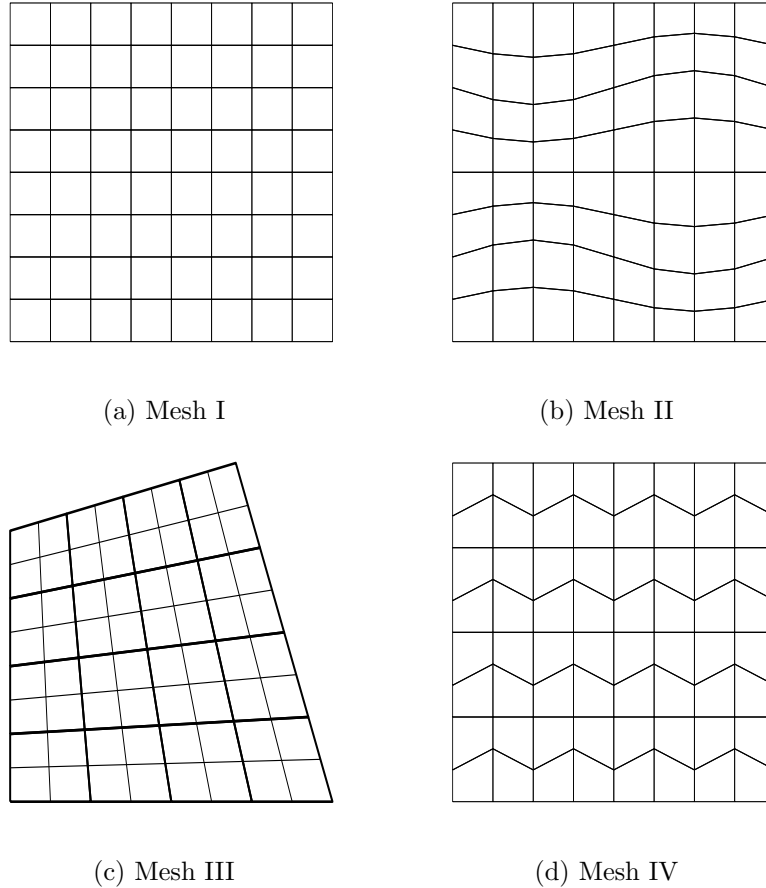


FIGURE 5. Four mesh types used in the numerical examples.

The analytic solution and corresponding right-hand side function are as follows

$$u(x, y) = \begin{cases} 2xe^y, & x \leq 0.5, \\ (0.5 + x)e^y, & x > 0.5, \end{cases} \quad f(x, y) = \begin{cases} -(2 + 3.5x)e^y, & x \leq 0.5, \\ -(3 + 2x)e^y, & x > 0.5. \end{cases}$$

Since Λ is discontinuous across the line $x = 0.5$, thus in this example we use Meshes I, II and IV. Although $u \notin W^{3,\infty}(\Omega)$ and has a lower regularity across the line $x = 0.5$, we can observe from Table 3 that the numerical performance is similar to the previous example, except the convergence orders of errors at the vertices and edge midpoints on Mesh II (a little lower than 2).

Example 3. Consider a highly anisotropic diffusion problem which was investigated in [39], where the diffusion tensor and exact solution are given by

$$\Lambda = \begin{pmatrix} \cos \theta & \sin \theta \\ -\sin \theta & \cos \theta \end{pmatrix} \begin{pmatrix} 1 & 0 \\ 0 & \kappa \end{pmatrix} \begin{pmatrix} \cos \theta & -\sin \theta \\ \sin \theta & \cos \theta \end{pmatrix}$$

and

$$u(x, y) = \frac{\arctan(0.5 - (x - 0.5)^2 - (y - 0.5)^2)}{\arctan 0.5},$$

TABLE 1. Numerical results for Example 1 on Meshes I and II.

Mesh	$\#\mathcal{T}_h$	8×8	16×16	32×32	64×64	128×128	256×256
Mesh I	ϱ	6.25e-02	6.25e-02	6.25e-02	6.25e-02	6.25e-02	6.25e-02
	$ u_I - u_h _1$	3.05e-03	8.23e-04	2.13e-04	5.38e-05	1.35e-05	3.39e-06
	Order	/	1.89	1.95	1.98	1.99	2.00
	$ u - u_h _1$	1.63e-01	8.15e-02	4.08e-02	2.04e-02	1.02e-02	5.09e-03
	Order	/	1.00	1.00	1.00	1.00	1.00
	$\ u - u_h\ _0$	9.21e-03	2.31e-03	5.79e-04	1.45e-04	3.62e-05	9.04e-06
	Order	/	1.99	2.00	2.00	2.00	2.00
	E_C	1.14e-02	2.86e-03	7.17e-04	1.79e-04	4.49e-05	1.12e-05
	Order	/	2.00	2.00	2.00	2.00	2.00
	E_V	1.12e-02	2.84e-03	7.15e-04	1.79e-04	4.49e-05	1.12e-05
	Order	/	1.98	1.99	2.00	2.00	2.00
	E_M	1.44e-02	3.61e-03	9.05e-04	2.26e-04	5.66e-05	1.42e-05
	Order	/	1.99	2.00	2.00	2.00	2.00
	Mesh II	ϱ	6.23e-02	6.24e-02	6.25e-02	6.25e-02	6.25e-02
$ u_I - u_h _1$		6.98e-03	2.19e-03	6.34e-04	1.70e-04	4.34e-05	1.09e-05
Order		/	1.67	1.79	1.90	1.97	1.99
$ u - u_h _1$		1.70e-01	8.52e-02	4.27e-02	2.13e-02	1.07e-02	5.33e-03
Order		/	0.99	1.00	1.00	1.00	1.00
$\ u - u_h\ _0$		9.18e-03	2.31e-03	5.79e-04	1.45e-04	3.63e-05	9.06e-06
Order		/	1.99	2.00	2.00	2.00	2.00
E_C		1.90e-02	4.93e-03	1.27e-03	3.23e-04	8.13e-05	2.04e-05
Order		/	1.95	1.95	1.98	1.99	2.00
E_V		2.73e-02	6.68e-03	1.67e-03	4.18e-04	1.05e-04	2.61e-05
Order		/	2.03	2.00	2.00	2.00	2.00
E_M		2.19e-02	5.89e-03	1.52e-03	3.86e-04	9.70e-05	2.43e-05
Order		/	1.90	1.95	1.98	1.99	2.00

respectively. As a result, the right-hand side function is as follows

$$f(x, y) = \frac{2}{(1 + f_1^2(x, y))^2 \arctan 0.5} \left((\kappa + 1) (1 + f_1^2(x, y)) + 8(\kappa - 1)(x - 0.5)(y - 0.5)f_1(x, y) \sin \theta \cos \theta + 4f_1(x, y) \left((x - 0.5)^2 (\kappa \sin^2 \theta + \cos^2 \theta) + (y - 0.5)^2 (\sin^2 \theta + \kappa \cos^2 \theta) \right) \right),$$

with $f_1(x, y) = x + y - x^2 - y^2$. Here, we set $\kappa = 10^3$ and $\theta = \pi/4$.

The numerical results are presented in Tables 4 and 5, and the performance is similar to Example 1, i.e., the convergence rates of errors validate the theoretical results in Theorem 3, Corollaries 1 and 2. Note that for the Mesh IV, the values of ϱ is negative. In other words, there exists a unique finite volume element solution that converges to exact solution with the desired convergence rates under H^1 and L^2 norms, even though the assumption (A1) not satisfied. This example shows that (A1) is just a sufficient condition to guarantee the coercivity.

Example 4. Solve the problem (1) and (2) with $\kappa = 1$, which allows the following exact solution

$$u(x, y) = x(1 - x)y(1 - y)r^{-\frac{3}{2}},$$

TABLE 2. Numerical results for Example 1 on Meshes III and IV.

Mesh	$\#\mathcal{T}_h$	8×8	16×16	32×32	64×64	128×128	256×256
Mesh III	ϱ	6.23e-02	6.24e-02	6.25e-02	6.25e-02	6.25e-02	6.25e-02
	$ u_I - u_h _1$	1.39e-03	3.73e-04	9.57e-05	2.42e-05	6.07e-06	1.52e-06
	Order	/	1.90	1.96	1.98	1.99	2.00
	$ u - u_h _1$	1.05e-01	5.25e-02	2.62e-02	1.31e-02	6.56e-03	3.28e-03
	Order	/	1.00	1.00	1.00	1.00	1.00
	$\ u - u_h\ _0$	4.85e-03	1.22e-03	3.04e-04	7.61e-05	1.90e-05	4.76e-06
	Order	/	2.00	2.00	2.00	2.00	2.00
	E_C	5.36e-03	1.35e-03	3.37e-04	8.44e-05	2.11e-05	5.28e-06
	Order	/	1.99	2.00	2.00	2.00	2.00
	E_V	7.54e-03	1.90e-03	4.78e-04	1.20e-04	3.00e-05	7.50e-06
	Order	/	1.99	1.99	2.00	2.00	2.00
	E_M	7.81e-03	1.96e-03	4.91e-04	1.23e-04	3.07e-05	7.68e-06
Order	/	1.99	2.00	2.00	2.00	2.00	
Mesh IV	ϱ	6.15e-02	6.15e-02	6.15e-02	6.15e-02	6.15e-02	6.15e-02
	$ u_I - u_h _1$	6.34e-03	2.17e-03	7.78e-04	3.27e-04	1.55e-04	7.62e-05
	Order	/	1.55	1.48	1.25	1.08	1.02
	$ u - u_h _1$	1.86e-01	9.42e-02	4.74e-02	2.38e-02	1.19e-02	5.95e-03
	Order	/	0.98	0.99	1.00	1.00	1.00
	$\ u - u_h\ _0$	1.02e-02	2.60e-03	6.57e-04	1.65e-04	4.14e-05	1.04e-05
	Order	/	1.97	1.99	1.99	2.00	2.00
	E_C	7.15e-02	3.55e-02	1.77e-02	8.84e-03	4.42e-03	2.21e-03
	Order	/	1.01	1.00	1.00	1.00	1.00
	E_V	1.55e-01	7.62e-02	3.78e-02	1.88e-02	9.38e-03	4.68e-03
	Order	/	1.02	1.01	1.01	1.00	1.00
	E_M	6.93e-02	3.50e-02	1.76e-02	8.81e-03	4.41e-03	2.21e-03
Order	/	0.99	0.99	1.00	1.00	1.00	

where $r = (x^2 + y^2)^{1/2}$. The source term f is obtained by u and κ accordingly. One can find that $u \in H^{3/2-\varepsilon}(\Omega)$, where $\varepsilon > 0$ is sufficiently small.

The numerical results are reported in Tables 6 and 7, one can see that the H^1 (resp. L^2) error order is 0.5 (resp. 1.5) for all four meshes. The reason is that, the exact solution has a lower regularity.

6. Conclusion

This work investigated the scheme that is obtained by using edge midpoint integral rule to approximate the line integrals in classical Q_1 -FVEM. Under **(A1)** and by element analysis technique, we proved the stability of the scheme. Specially, we find that **(A1)** covers $h^{1+\gamma}$ -parallelogram and some trapezoidal meshes with any full anisotropic diffusion tensor. Based on the coercivity result and suppose that the quadrilateral mesh is h^2 -uniform, we proved the superconvergence $|u_I - u_h|_1 = \mathcal{O}(h^2)$, which leads to $|u - u_h|_1 = \mathcal{O}(h)$ and $\|u - u_h\|_0 = \mathcal{O}(h^2)$. Further, the superconvergence results of u_h at geometric centers, interior vertices and edge midpoints are also obtained in an average gradient norm. Thus, we improved the theoretical results in [17].

We mention that the numerical results in Example 3 indicate that, there exists a unique finite volume element solution that converges to exact solution with the

TABLE 3. Numerical results for Example 2.

Mesh	$\#\mathcal{T}_h$	8×8	16×16	32×32	64×64	128×128	256×256
Mesh I	ϱ	1.76e-01	1.76e-01	1.76e-01	1.76e-01	1.76e-01	1.76e-01
	$ u_I - u_h _1$	1.81e-03	4.67e-04	1.18e-04	2.95e-05	7.39e-06	1.85e-06
	Order	/	1.95	1.99	2.00	2.00	2.00
	$ u - u_h _1$	6.33e-02	3.16e-02	1.58e-02	7.89e-03	3.95e-03	1.97e-03
	Order	/	1.00	1.00	1.00	1.00	1.00
	$\ u - u_h\ _0$	2.76e-03	6.93e-04	1.73e-04	4.34e-05	1.08e-05	2.71e-06
	Order	/	1.99	2.00	2.00	2.00	2.00
	E_C	6.19e-03	1.56e-03	3.90e-04	9.75e-05	2.44e-05	6.09e-06
	Order	/	1.99	2.00	2.00	2.00	2.00
	E_V	4.59e-03	1.16e-03	2.90e-04	7.27e-05	1.82e-05	4.55e-06
	Order	/	1.99	1.99	2.00	2.00	2.00
	E_M	5.43e-03	1.37e-03	3.43e-04	8.59e-05	2.15e-05	5.38e-06
Order	/	1.99	2.00	2.00	2.00	2.00	
Mesh II	ϱ	1.75e-01	1.76e-01	1.76e-01	1.76e-01	1.76e-01	1.76e-01
	$ u_I - u_h _1$	6.72e-03	2.03e-03	5.35e-04	1.36e-04	3.40e-05	8.51e-06
	Order	/	1.73	1.92	1.98	1.99	2.00
	$ u - u_h _1$	7.25e-02	3.63e-02	1.82e-02	9.09e-03	4.54e-03	2.27e-03
	Order	/	1.00	1.00	1.00	1.00	1.00
	$\ u - u_h\ _0$	3.50e-03	9.06e-04	2.29e-04	5.73e-05	1.43e-05	3.59e-06
	Order	/	1.95	1.99	2.00	2.00	2.00
	E_C	1.63e-02	4.41e-03	1.13e-03	2.84e-04	7.10e-05	1.78e-05
	Order	/	1.88	1.97	1.99	2.00	2.00
	E_V	2.89e-02	7.60e-03	2.04e-03	5.75e-04	1.72e-04	5.48e-05
	Order	/	1.93	1.90	1.83	1.74	1.65
	E_M	2.12e-02	6.07e-03	1.65e-03	4.56e-04	1.33e-04	4.09e-05
Order	/	1.80	1.88	1.85	1.78	1.70	
Mesh IV	ϱ	1.73e-01	1.73e-01	1.73e-01	1.73e-01	1.73e-01	1.73e-01
	$ u_I - u_h _1$	7.61e-03	4.03e-03	2.10e-03	1.07e-03	5.44e-04	2.74e-04
	Order	/	0.92	0.94	0.97	0.98	0.99
	$ u - u_h _1$	9.88e-02	4.94e-02	2.47e-02	1.24e-02	6.18e-03	3.09e-03
	Order	/	1.00	1.00	1.00	1.00	1.00
	$\ u - u_h\ _0$	4.05e-03	1.04e-03	2.63e-04	6.62e-05	1.66e-05	4.15e-06
	Order	/	1.96	1.98	1.99	2.00	2.00
	E_C	5.32e-02	2.66e-02	1.33e-02	6.67e-03	3.34e-03	1.67e-03
	Order	/	1.00	1.00	1.00	1.00	1.00
	E_V	1.35e-01	6.57e-02	3.24e-02	1.61e-02	8.02e-03	4.00e-03
	Order	/	1.04	1.02	1.01	1.00	1.00
	E_M	6.18e-02	3.12e-02	1.57e-02	7.84e-03	3.92e-03	1.96e-03
Order	/	0.99	1.00	1.00	1.00	1.00	

desired convergence orders under H^1 and L^2 norms, even though (A1) is violated. Therefore, a more general assumption weaker than (A1), is worth to be considered in future work. Moreover, extending the relevant theoretical results to hexahedral mesh is also a valuable work. To this end, similar to the notations (18) and (19) in 2D, we also need to suggest some special symbols to express the element stiffness

TABLE 4. Numerical results for Example 3 on Meshes I and II.

Mesh	$\#\mathcal{T}_h$	8×8	16×16	32×32	64×64	128×128	256×256
Mesh I	ϱ	6.25e+01	6.25e+01	6.25e+01	6.25e+01	6.25e+01	6.25e+01
	$ u_I - u_h _1$	3.70e-03	1.29e-03	3.86e-04	1.09e-04	2.94e-05	7.72e-06
	Order	/	1.52	1.74	1.83	1.89	1.93
	$ u - u_h _1$	2.14e-01	1.07e-01	5.36e-02	2.68e-02	1.34e-02	6.69e-03
	Order	/	1.00	1.00	1.00	1.00	1.00
	$\ u - u_h\ _0$	1.15e-02	2.87e-03	7.15e-04	1.79e-04	4.46e-05	1.12e-05
	Order	/	2.01	2.00	2.00	2.00	2.00
	E_C	5.92e-03	1.82e-03	5.10e-04	1.37e-04	3.62e-05	9.35e-06
	Order	/	1.70	1.84	1.89	1.93	1.95
	E_V	1.09e-02	2.93e-03	7.63e-04	1.97e-04	5.04e-05	1.28e-05
	Order	/	1.90	1.94	1.95	1.97	1.98
	E_M	9.35e-03	2.62e-03	6.98e-04	1.82e-04	4.69e-05	1.19e-05
	Order	/	1.83	1.91	1.94	1.96	1.97
	Mesh II	ϱ	2.34e+01	4.91e+01	5.89e+01	6.16e+01	6.23e+01
$ u_I - u_h _1$		3.88e-02	1.62e-02	5.25e-03	1.53e-03	4.11e-04	1.06e-04
Order		/	1.26	1.62	1.78	1.89	1.96
$ u - u_h _1$		2.24e-01	1.12e-01	5.57e-02	2.78e-02	1.39e-02	6.94e-03
Order		/	1.00	1.01	1.00	1.00	1.00
$\ u - u_h\ _0$		1.30e-02	3.57e-03	9.48e-04	2.44e-04	6.19e-05	1.56e-05
Order		/	1.86	1.91	1.96	1.98	1.99
E_C		4.55e-02	1.77e-02	5.55e-03	1.58e-03	4.23e-04	1.08e-04
Order		/	1.36	1.67	1.81	1.91	1.96
E_V		4.94e-02	1.85e-02	5.69e-03	1.61e-03	4.27e-04	1.09e-04
Order		/	1.42	1.70	1.82	1.91	1.97
E_M		4.62e-02	1.80e-02	5.62e-03	1.60e-03	4.26e-04	1.09e-04
Order		/	1.36	1.68	1.82	1.91	1.97

matrix in 3D. In summary, more detailed analysis is required to analyze the positive definiteness of the element matrix on hexahedral mesh.

7. Acknowledgments

The author would like to thank the reviewers for their carefully readings and providing some insightful comments and suggestions, that lead to an improvement of the presentation. This work was partially supported by the National Natural Science Foundation of China (No. 12401517), Opening Project of Guangdong Province Key Laboratory of Computational Science at the Sun Yat-sen University (No. 2024006) and LCP Fund for Young Scholar (No. 6142A05QN23008).

8. Appendix A: Some lemmas available in the literature.

This section presents some lemmas that almost available in the literature.

Lemma 8. For the $\bar{\beta}_K$ and $\bar{\gamma}_K$ defined by (13), we have

$$(39) \quad \mathbf{m}_K = \bar{\gamma}_K \mathbf{m}_1 + \bar{\beta}_K \mathbf{m}_2,$$

and

$$(40) \quad |\bar{\beta}_K| + |\bar{\gamma}_K| < 1,$$

TABLE 5. Numerical results for Example 3 on Meshes III and IV.

Mesh	$\#\mathcal{T}_h$	8×8	16×16	32×32	64×64	128×128	256×256
Mesh III	ϱ	5.76e+01	6.12e+01	6.22e+01	6.24e+01	6.25e+01	6.25e+01
	$ u_I - u_h _1$	3.78e-03	1.21e-03	3.34e-04	8.73e-05	2.23e-05	5.65e-06
	Order	/	1.64	1.86	1.94	1.97	1.98
	$ u - u_h _1$	1.68e-01	8.40e-02	4.20e-02	2.10e-02	1.05e-02	5.25e-03
	Order	/	1.00	1.00	1.00	1.00	1.00
	$\ u - u_h\ _0$	8.02e-03	2.00e-03	5.00e-04	1.25e-04	3.13e-05	7.82e-06
	Order	/	2.00	2.00	2.00	2.00	2.00
	E_C	8.97e-03	2.44e-03	6.34e-04	1.61e-04	4.07e-05	1.02e-05
	Order	/	1.88	1.95	1.98	1.99	1.99
	E_V	9.50e-03	2.56e-03	6.60e-04	1.68e-04	4.22e-05	1.06e-05
	Order	/	1.89	1.95	1.98	1.99	1.99
	E_M	9.86e-03	2.70e-03	7.00e-04	1.78e-04	4.49e-05	1.13e-05
Order	/	1.87	1.94	1.98	1.99	1.99	
Mesh IV	ϱ	-1.82e+02	-1.82e+02	-1.82e+02	-1.82e+02	-1.82e+02	-1.82e+02
	$ u_I - u_h _1$	1.45e-02	7.39e-03	3.73e-03	1.88e-03	9.45e-04	4.74e-04
	Order	/	0.97	0.99	0.99	0.99	1.00
	$ u - u_h _1$	2.29e-01	1.15e-01	5.73e-02	2.87e-02	1.43e-02	7.17e-03
	Order	/	1.00	1.00	1.00	1.00	1.00
	$\ u - u_h\ _0$	1.31e-02	3.25e-03	8.11e-04	2.02e-04	5.06e-05	1.26e-05
	Order	/	2.01	2.00	2.00	2.00	2.00
	E_C	6.55e-02	3.28e-02	1.64e-02	8.21e-03	4.11e-03	2.05e-03
	Order	/	1.00	1.00	1.00	1.00	1.00
	E_V	6.71e-02	3.34e-02	1.67e-02	8.34e-03	4.17e-03	2.09e-03
	Order	/	1.01	1.00	1.00	1.00	1.00
	E_M	1.63e-02	7.01e-03	3.28e-03	1.61e-03	7.98e-04	3.99e-04
Order	/	1.22	1.10	1.03	1.01	1.00	

Further, for the m_{ij} appeared in (18)

$$(41) \quad m_{ii} > 0, \quad m_{12} = m_{21}, \quad m_{11}m_{22} - m_{12}^2 = \frac{1}{16} \det(\Lambda),$$

and under the assumption (12)

$$(42) \quad m_{ii} < \frac{\bar{\lambda}C_r}{2\pi}, \quad i = 1, 2.$$

Proof. The proof of (39), (40) and (41) can be found in Lemmas 3.1 and 3.2 of [24]. By (3) and (12), we have

$$m_{ii} \leq \frac{\bar{\lambda} \|\mathbf{m}_i\|^2}{4|K|} < \frac{\bar{\lambda} h_K^2}{8\pi \left(\frac{\rho_K}{2}\right)^2} \leq \frac{\bar{\lambda}C_r}{2\pi}, \quad i = 1, 2,$$

which leads to (42). The proof is complete. □

Lemma 9 (Lemma 5 of [22]). *For the matrix \mathbb{T} defined by (25), we have*

$$(43) \quad \|\mathbb{T}\| < \frac{17}{8},$$

where $\|\mathbb{T}\|$ is the spectral norm of \mathbb{T} .

TABLE 6. Numerical results for Example 4 on Meshes I and II.

Mesh	$\#\mathcal{T}_h$	8×8	16×16	32×32	64×64	128×128	256×256
Mesh I	ρ	6.25e-02	6.25e-02	6.25e-02	6.25e-02	6.25e-02	6.25e-02
	$ u_I - u_h _1$	1.88e-02	1.21e-02	8.18e-03	5.65e-03	3.95e-03	2.78e-03
	Order	/	0.63	0.57	0.53	0.52	0.51
	$ u - u_h _1$	2.51e-01	1.85e-01	1.33e-01	9.52e-02	6.77e-02	4.80e-02
	Order	/	0.44	0.47	0.48	0.49	0.50
	$\ u - u_h\ _0$	9.59e-03	3.53e-03	1.27e-03	4.53e-04	1.61e-04	5.70e-05
	Order	/	1.44	1.47	1.49	1.49	1.50
	E_C	6.75e-02	4.94e-02	3.58e-02	2.56e-02	1.83e-02	1.30e-02
	Order	/	0.45	0.47	0.48	0.49	0.49
	E_V	8.76e-02	5.97e-02	4.15e-02	2.91e-02	2.05e-02	1.45e-02
	Order	/	0.55	0.52	0.51	0.51	0.50
	E_M	8.95e-02	6.36e-02	4.53e-02	3.22e-02	2.28e-02	1.61e-02
	Order	/	0.49	0.49	0.49	0.50	0.50
	Mesh II	ρ	6.23e-02	6.24e-02	6.25e-02	6.25e-02	6.25e-02
$ u_I - u_h _1$		1.63e-02	1.11e-02	7.67e-03	5.42e-03	3.86e-03	2.74e-03
Order		/	0.56	0.53	0.50	0.49	0.49
$ u - u_h _1$		2.60e-01	1.89e-01	1.35e-01	9.60e-02	6.80e-02	4.82e-02
Order		/	0.46	0.48	0.49	0.50	0.50
$\ u - u_h\ _0$		1.06e-02	3.75e-03	1.31e-03	4.59e-04	1.62e-04	5.72e-05
Order		/	1.49	1.52	1.51	1.50	1.50
E_C		6.93e-02	4.77e-02	3.45e-02	2.51e-02	1.80e-02	1.29e-02
Order		/	0.54	0.46	0.46	0.48	0.49
E_V		8.41e-02	5.68e-02	4.01e-02	2.85e-02	2.03e-02	1.44e-02
Order		/	0.57	0.50	0.49	0.49	0.49
E_M		8.40e-02	5.98e-02	4.35e-02	3.15e-02	2.25e-02	1.61e-02
Order		/	0.49	0.46	0.47	0.48	0.49

Lemma 10 (Proposition 1 of [18]). *Assume that \mathcal{T}_h is regular, then there exist two positive constants \underline{C} and \overline{C} such that*

$$(44) \quad \underline{C}|u_h|_{1,K,h} \leq |u_h|_{1,K} \leq \overline{C}|u_h|_{1,K,h}, \quad \forall u_h \in U_h, \quad \forall K \in \mathcal{T}_h,$$

where $|u_h|_{1,K,h} = \|\delta U_K\|$.

Lemma 11. *Assume that \mathcal{T}_h is h^2 -uniform, then we have*

$$(45) \quad \|\overline{\nabla}(u - u_I)(\mathbf{x})\| \lesssim h^2 \|u\|_{3,\infty}, \quad \forall u \in W^{3,\infty}(\Omega),$$

where $\overline{\nabla}$ is the arithmetic average of the gradient over all neighbouring quadrilateral elements for \mathbf{x} , while \mathbf{x} is any geometric center in \mathcal{C}_h , or any interior vertex in \mathcal{N}_h° , or any interior midpoint in \mathcal{M}_h° .

Proof. The superconvergence of finite element method has been studied in some references (cf. [40, 41]), and the proof of (45) can be found in Theorem 1 of [38]. \square

9. Appendix B: Some discussions for (A1)

From Theorem 1, we find that the assumption (A1) is critical to the coercivity result of Q_1 -FVEM-EM scheme. However, the meaning of the left-hand side in (20) is not so straightforward. In this section, we employ some special meshes to

TABLE 7. Numerical results for Example 4 on Meshes III and IV.

Mesh	$\#\mathcal{T}_h$	8×8	16×16	32×32	64×64	128×128	256×256
Mesh III	ϱ	6.25e-02	6.25e-02	6.25e-02	6.25e-02	6.25e-02	6.25e-02
	$ u_I - u_h _1$	1.78e-02	1.16e-02	7.80e-03	5.39e-03	3.77e-03	2.65e-03
	Order	/	0.62	0.57	0.53	0.52	0.51
	$ u - u_h _1$	2.43e-01	1.78e-01	1.29e-01	9.19e-02	6.54e-02	4.64e-02
	Order	/	0.45	0.47	0.48	0.49	0.50
	$\ u - u_h\ _0$	8.22e-03	3.05e-03	1.10e-03	3.94e-04	1.40e-04	4.97e-05
	Order	/	1.43	1.47	1.48	1.49	1.50
	E_C	8.85e-02	6.71e-02	4.94e-02	3.56e-02	2.55e-02	1.81e-02
	Order	/	0.40	0.44	0.47	0.48	0.49
	E_V	9.46e-02	6.45e-02	4.49e-02	3.16e-02	2.23e-02	1.57e-02
	Order	/	0.55	0.52	0.51	0.50	0.50
	E_M	9.54e-02	6.72e-02	4.76e-02	3.37e-02	2.39e-02	1.69e-02
	Order	/	0.51	0.50	0.50	0.50	0.50
	Mesh IV	ϱ	6.15e-02	6.15e-02	6.15e-02	6.15e-02	6.15e-02
$ u_I - u_h _1$		1.61e-02	1.10e-02	7.74e-03	5.51e-03	3.92e-03	2.78e-03
Order		/	0.55	0.51	0.49	0.49	0.49
$ u - u_h _1$		2.60e-01	1.91e-01	1.37e-01	9.81e-02	6.98e-02	4.95e-02
Order		/	0.45	0.47	0.48	0.49	0.50
$\ u - u_h\ _0$		1.02e-02	3.75e-03	1.35e-03	4.83e-04	1.72e-04	6.09e-05
Order		/	1.44	1.47	1.49	1.49	1.50
E_C		8.05e-02	6.07e-02	4.46e-02	3.22e-02	2.31e-02	1.64e-02
Order		/	0.41	0.44	0.47	0.48	0.49
E_V		9.03e-02	6.48e-02	4.69e-02	3.38e-02	2.42e-02	1.73e-02
Order		/	0.48	0.47	0.47	0.48	0.49
E_M		8.54e-02	6.03e-02	4.30e-02	3.06e-02	2.18e-02	1.54e-02
Order		/	0.50	0.49	0.49	0.49	0.49

explore the meaning of (A1), including the parallelogram, $h^{1+\gamma}$ -parallelogram and trapezoidal meshes.

9.1. Parallelogram mesh.

Theorem 4. Assume that \mathcal{T}_h consists of parallelograms, then (A1) holds with

$$(46) \quad \varrho = \min_{K \in \mathcal{T}_h} \left[\frac{1}{16} \det(\Lambda) \right] \geq \frac{1}{16} \lambda^2.$$

Proof. Since $K \in \mathcal{T}_h$ is a parallelogram, then we have $\mathbf{m}_K = \mathbf{0}$, $\bar{\beta}_K = \bar{\gamma}_K = 0$. By (19), (41) and (3), we find that

$$\zeta_1 \zeta_2 - m_{12}^2 = m_{11} m_{22} - m_{12}^2 = \frac{1}{16} \det(\Lambda) \geq \frac{1}{16} \lambda^2, \quad \forall K \in \mathcal{T}_h,$$

which implies (46). □

9.2. $h^{1+\gamma}$ -parallelogram mesh. We call \mathcal{T}_h is an $h^{1+\gamma}$ -parallelogram mesh provided that there exists a positive constant C independent of K and h , such that

$$(47) \quad \|\mathbf{m}_K\| \leq Ch_K^{1+\gamma}, \quad \forall K \in \mathcal{T}_h,$$

where $\gamma > 0$ is a constant.

Theorem 5. Assume that \mathcal{T}_h is regular and consists of $h^{1+\gamma}$ -parallelograms. Then, when the mesh size h small enough, we have

$$\left| (\zeta_1 \zeta_2 - m_{12}^2) - \frac{1}{16} \det(\Lambda) \right| \leq Ch_K^{2\gamma}, \quad \forall K \in \mathcal{T}_h.$$

As a result, (A1) holds with $\varrho = C_0 \lambda^2$, where $0 < C_0 < 1/16$ is a constant.

Proof. For simplicity, we denote

$$a_1 = -\frac{1}{8} \mu_2 \bar{\beta}_K^2, \quad a_2 = -\frac{1}{8} \mu_1 \bar{\gamma}_K^2.$$

It follows from (19) and (41) that

$$\zeta_1 \zeta_2 - m_{12}^2 = (m_{11} + a_1)(m_{22} + a_2) - m_{12}^2 = \frac{1}{16} \det(\Lambda) + Res,$$

where

$$Res = a_2 m_{11} + a_1 m_{22} + a_1 a_2.$$

By (13), (12) and (47)

$$\max \{ |\bar{\beta}_K|, |\bar{\gamma}_K| \} < \frac{Ch_K^{2+\gamma}}{2\pi \left(\frac{\rho_K}{2}\right)^2} \leq \frac{2C_r^2 C}{\pi} h_K^\gamma,$$

and when h is small enough, we have

$$\max\{\mu_1, \mu_2\} < 4 \max\{m_{11}, m_{22}\} < \frac{2\bar{\lambda}C_r}{\pi}.$$

It holds that

$$\max_{i=1,2} |a_i| < \frac{\bar{\lambda}C_r^5 C^2}{\pi^3} h_K^{2\gamma}.$$

Consequently, there exists a positive constant C such that $|Res| \leq Ch_K^{2\gamma}$. The proof is complete. \square

9.3. Trapezoidal mesh.

Theorem 6. Assume that \mathcal{T}_h consists of trapezoids, i.e., for each K , there holds $\bar{\beta}_K = 0$ or $\bar{\gamma}_K = 0$. Then, we have the following results.

(i) If $\bar{\beta}_K = 0$, the assumption (A1) holds if and only if

$$\frac{\det(\Lambda) - 4m_{11}^2 \bar{\gamma}_K^2}{16} \geq \varrho, \quad \forall K \in \mathcal{T}_h.$$

(ii) If $\bar{\gamma}_K = 0$, the assumption (A1) holds if and only if

$$\frac{\det(\Lambda) - 4m_{22}^2 \bar{\beta}_K^2}{16} \geq \varrho, \quad \forall K \in \mathcal{T}_h.$$

Proof. If $\bar{\beta}_K = 0$, then we deduce from (19), (18) and (41) that

$$(48) \quad \zeta_1 \zeta_2 - m_{12}^2 = m_{11} \left(m_{22} - \frac{1}{8} \mu_1 \bar{\gamma}_K^2 \right) - m_{12}^2 = \frac{1}{16} \det(\Lambda) - \frac{1}{4} m_{11}^2 \bar{\gamma}_K^2,$$

which leads to the first part of this theorem. Similarly, if $\bar{\gamma}_K = 0$, we have

$$\zeta_1 \zeta_2 - m_{12}^2 = m_{22} \left(m_{11} - \frac{1}{8} \mu_2 \bar{\beta}_K^2 \right) - m_{12}^2 = \frac{1}{16} \det(\Lambda) - \frac{1}{4} m_{22}^2 \bar{\beta}_K^2,$$

implies the second part of this theorem. The proof is complete. \square

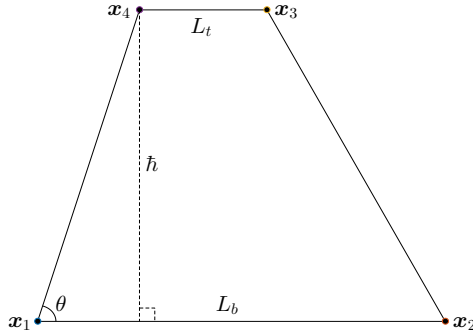


FIGURE 6. A general trapezoidal element used in Corollary 3.

Corollary 3. Assume that $\Lambda = \mathbb{I}$ is the identity matrix and \mathcal{T}_h consists of trapezoids. For each trapezoidal element K , let L_b , L_t and h be its lengths of the bottom, top and height, see Figure 6. Then, we have the following results.

(i) \mathbb{B}_K is a positive definite matrix if and only if

$$(49) \quad \frac{|L_b - L_t|}{h} < 4.$$

(ii) If

$$(50) \quad \frac{|L_b - L_t|}{h} \leq 4 - \tau$$

holds, where $0 < \tau < 4$ is a constant, independent of K and h , then the assumption **(A1)** holds with

$$\varrho = \frac{1}{256} \tau(8 - \tau).$$

Proof. For simplicity, we denote

$$\tau_b = \frac{L_b}{h}, \quad \tau_t = \frac{L_t}{h},$$

and assume that the coordinates of K are given by

$$\mathbf{x}_1 = (0, 0)^T, \quad \mathbf{x}_2 = (\tau_b h, 0)^T, \quad \mathbf{x}_3 = (h \cot \theta + \tau_t h, h)^T, \quad \mathbf{x}_4 = (h \cot \theta, h)^T,$$

where θ is the interior angle at the bottom-left corner. A direct calculation yields that

$$|K| = \frac{1}{2} h^2 (\tau_b + \tau_t), \quad \bar{\beta}_K = 0, \quad \bar{\gamma}_K = \frac{\tau_t - \tau_b}{\tau_b + \tau_t}, \quad m_{11} = \frac{1}{8} (\tau_b + \tau_t).$$

It follows from (48) that

$$(51) \quad \zeta_1 \zeta_2 - m_{12}^2 = \frac{1}{256} [16 - (\tau_b - \tau_t)^2].$$

As a result, \mathbb{B}_K is a positive definite matrix if and only if $|\tau_b - \tau_t| < 4$, which implies (49). Further, (50) is equivalent to $|\tau_b - \tau_t| \leq 4 - \tau$. Therefore, if (50) holds, then we deduce from (51) that

$$\zeta_1 \zeta_2 - m_{12}^2 \geq \frac{1}{256} [16 - (4 - \tau)^2] = \frac{1}{256} \tau(8 - \tau).$$

The proof is complete. □

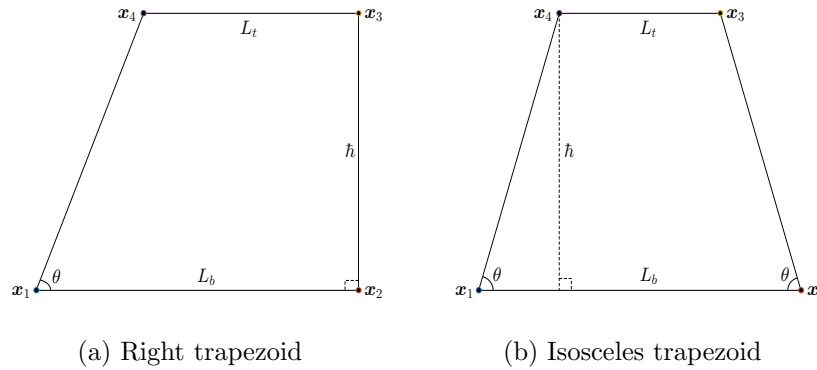


FIGURE 7. Two special trapezoidal elements used in Remark 3.

Remark 3. For some special trapezoidal element, we have the following results.

(i) If K is a right trapezoid, see Figure 7(a), then (49) reduces to the following acute angle condition

$$\theta > \arctan \frac{1}{4} \approx 14.036^\circ,$$

which is a little bigger than the 10.025° in [22].

(ii) If K is an isosceles trapezoid, see Figure 7(b), then (49) reduces to the following acute angle condition

$$\theta > \arctan \frac{1}{2} \approx 26.565^\circ,$$

which is also a little bigger than the 19.471° in [22].

In fact, it can be checked that the assumption **(A1)** suggested in this paper is a little stronger than that of [22].

References

- [1] R. Li, P. Zhu: Generalized difference methods for second order elliptic partial differential equations (I)-triangle grids (in Chinese). Numer. Math. J. Chin. Univ., 2, 140-152 (1982).
- [2] R. E. Bank, D. J. Rose: Some error estimates for the box method. SIAM J. Numer. Anal., 24, 777-787 (1987).
- [3] R. Li, Z. Chen, W. Wu: Generalized difference methods for differential equations: Numerical analysis of finite volume methods. Marcel Dekker, New York (2000).
- [4] Y. Lin, J. Liu, M. Yang: Finite volume element methods: an overview on recent developments. Int. J. Numer. Anal. Mod. B, 4, 14-34 (2013).
- [5] Z. Zhang, Q. Zou: Some recent advances on vertex centered finite volume element methods for elliptic equations. Sci. China Math., 56, 2507-2522 (2013).
- [6] Z. Cai: On the finite volume element method. Numer. Math., 58, 713-735 (1991).
- [7] J. Xu, Q. Zou: Analysis of linear and quadratic simplicial finite volume methods for elliptic equations. Numer. Math., 111, 469-492 (2009).
- [8] Z. Chen, R. Li, A. Zhou: A note on the optimal L^2 -estimate of the finite volume element method. Adv. Comput. Math., 16, 291-303 (2002).
- [9] R. E. Ewing, T. Lin, Y. Lin: On the accuracy of the finite volume element method based on piecewise linear polynomials. SIAM J. Numer. Anal., 39, 1865-1888 (2002).
- [10] S. Karaa, K. Mustapha, A. Pani: Finite volume element method for two-dimensional fractional subdiffusion problems. IMA J. Numer. Anal., 37, 945-964 (2017).
- [11] C. Erath, D. Praetorius: Adaptive vertex-centered finite volume methods for general second-order linear elliptic partial differential equations. IMA J. Numer. Anal., 39, 983-1008 (2019).
- [12] Z. Chen, J. Wu, Y. Xu: Higher-order finite volume methods for elliptic boundary value problems. Adv. Comput. Math., 37, 191-253 (2012).

- [13] X. Wang, Y. Li: L^2 error estimates for high order finite volume methods on triangular meshes. *SIAM J. Numer. Anal.*, 54, 2729-2749 (2016).
- [14] Q. Zou: An unconditionally stable quadratic finite volume scheme over triangular meshes for elliptic equations. *J. Sci. Comput.*, 70, 112-124 (2017).
- [15] Y. Zhou, J. Wu: A family of quadratic finite volume element schemes for anisotropic diffusion problems on triangular meshes. *J. Comput. Appl. Math.*, 402, 113794 (2022).
- [16] X. Wen, Y. Zhou: A coercivity result of quadratic finite volume element schemes over triangular meshes. *Adv. Appl. Math. Mech.*, 15, 901-931 (2023).
- [17] P. Zhu, R. Li: Generalized difference methods for second order elliptic partial differential equations. II. Quadrilateral subdivision (in Chinese). *Numer. Math. J. Chin. Univ.*, 4, 360-375 (1982).
- [18] Y. Li, R. Li: Generalized difference methods on arbitrary quadrilateral networks. *J. Comput. Math.*, 17, 653-672 (1999).
- [19] Z. Zhang, Q. Zou: Vertex-centered finite volume schemes of any order over quadrilateral meshes for elliptic boundary value problems. *Numer. Math.*, 130, 363-393 (2015).
- [20] Q. Hong, J. Wu: A Q_1 -finite volume element scheme for anisotropic diffusion problems on general convex quadrilateral mesh. *J. Comput. Appl. Math.*, 372, 112732 (2020).
- [21] S. Shu, H. Yu, Y. Huang, C. Nie: A symmetric finite volume element scheme on quadrilateral grids and superconvergence. *Int. J. Numer. Anal. Mod.*, 3, 348-360 (2006).
- [22] Q. Hong, J. Wu: Coercivity results of a modified Q_1 -finite volume element scheme for anisotropic diffusion problems. *Adv. Comput. Math.*, 44, 897-922 (2018).
- [23] F. Fang, Q. Hong, J. Wu: Analysis of a special Q_1 -finite volume element scheme for anisotropic diffusion problems. *Numer. Math. Theor. Meth. Appl.*, 12, 1141-1167 (2019).
- [24] S. Mu, Y. Zhou: An analysis of the isoparametric bilinear finite volume element method by applying the Simpson rule to quadrilateral meshes. *AIMS Math.*, 8, 22507-22537 (2023).
- [25] Y. Zhou, Y. Zhang, J. Wu: A polygonal finite volume element method for anisotropic diffusion problems. *Comput. Math. Appl.*, 140, 225-236 (2023).
- [26] Y. Lin, M. Yang, Q. Zou: L^2 error estimates for a class of any order finite volume schemes over quadrilateral meshes. *SIAM J. Numer. Anal.*, 53, 2030-2050 (2015).
- [27] W. He, Z. Zhang, Q. Zou: Maximum-norms error estimates for high-order finite volume schemes over quadrilateral meshes. *Numer. Math.*, 138, 473-500 (2018).
- [28] Y. Zhou, J. Wu: A new high order finite volume element solution on arbitrary triangular and quadrilateral meshes. *Appl. Math. Lett.*, 134, 108354 (2022).
- [29] Y. Zhang, X. Wang: Unified construction and L^2 analysis for the finite volume element method over tensorial meshes. *Adv. Comput. Math.*, 49, 2 (2023).
- [30] W. Hackbusch: On first and second order box schemes. *Computing*, 41, 277-296 (1989).
- [31] J. Lv, Y. Li: L^2 error estimates and superconvergence of the finite volume element methods on quadrilateral meshes. *Adv. Comput. Math.*, 37, 393-416 (2012).
- [32] S. Chou, X. Ye: Superconvergence of finite volume methods for the second order elliptic problem. *Comput. Methods Appl. Mech. Eng.*, 196, 3706-3712 (2007)
- [33] T. Wang, Y. Gu: Superconvergent biquadratic finite volume element method for two-dimensional Poisson's equations. *J. Comput. Appl. Math.*, 234, 447-460 (2010).
- [34] W. Cao, Z. Zhang, Q. Zou: Is $2k$ -Conjecture valid for finite volume methods? *SIAM J. Numer. Anal.*, 53, 942-962 (2015).
- [35] Y. Zhou, Y. Jiang, Q. Zou: Three dimensional high order finite volume element schemes for elliptic equations. *Numer. Methods Partial Differ. Eq.*, 39, 1672-1705 (2023).
- [36] S. Chou, S. He: On the regularity and uniformness conditions on quadrilateral grids. *Comput. Methods Appl. Mech. Engrg.*, 191, 5149-5158 (2002).
- [37] R. Ewing, M. Liu, J. Wang: Superconvergence of mixed finite element approximations over quadrilaterals. *SIAM J. Numer. Anal.*, 36, 772-787 (1999).
- [38] L. Zhang, L. Li: On superconvergence of isoparametric bilinear finite elements. *Comm. Numer. Methods Engrg.*, 12, 849-862 (1996).
- [39] J. Camier, F. Hermeline: A monotone nonlinear finite volume method for approximating diffusion operators on general meshes. *Int. J. Numer. Meth. Engrg.*, 107, 496-519 (2016).
- [40] P. Lesaint, M. Zlámal: Superconvergence of the gradient of finite element solutions. *RAIRO Anal. Numér.*, 13, 139-166 (1979).
- [41] Q. Zhu, Q. Lin: Superconvergence Theory for Finite Element Methods (in Chinese). Hunan Science and Technology Press, Changsha (1989).

School of Mathematics and Systems Science, Guangdong Polytechnic Normal University, Guangzhou,
510665, China

E-mail: zhouyh9@mail2.sysu.edu.cn